Characterization of ligninolytic enzymes and metabolic profile of *Cryphonectria parasitica* and the isogenic converted strains by CHV1 hypovirus

Omar Abdelaziz Ouni

Dissertation presented to the Polytechnic Institute of Bragança to obtain the master's degree in Biotechnological Engineering within the Double Diploma with Université Libre de Tunis

Supervised by

Professor Eugénia Gouveia

Professor Lurdes Jorge

Professor Fériel Rezouga

Bragança

2019

Abstract

Cryphonectria parasitica, the causal agent of Chestnut Blight, causes necrotic lesions (so-called cankers) on the bark of stems and branches of susceptible host trees. *Cryphonectria* Hypovirus 1 (CHV1) infects *C. parasitica* and reduces the fungus virulence (hypovirulence) and alters the fungus morphology in culture (pigmentation and sporulation capacity). By these characteristics the mycovirus CHV1 is used in Europe as a biological control agent of Chestnut Blight. The aim of this project is to better understand the effect of the mycovirus on the fungi pathogenicity by comparing the production of some lignin degrading enzymes and the metabolic profiles of some virulent and hypovirulent (converted and original) strains. For qualitative evaluation, several different compounds have been used as indicators for ligninolytic enzymes production. For quantitative evaluation, among nine strains five were chosen for biological tests and cultivation in minimal liquid media and the amount of enzyme produced were analyzed. Virulent strains were found to cause more damage in chestnut branches and to produce more lignin degrading enzymes. In apple fruits, some CHV1 infected strains produced bigger rot lesions than wild type strains. In parallel, Biolog FF MicroPlates have been used for the first time with *C. parasitica* strains to assess their metabolic profiles with concurrent reads of utilization of 95 different carbon sources. Moreover, carbohydrates, amino acids, amines/amides, miscellaneous and polymers were found to be more consumed by hypovirulent strains; therefore, this may suggest a novel adaptation mechanism in fungal ecology and fitness.

Keywords: *Cryphonectria parasitica*, Chestnut Blight, Hypovirulence, Lignin degrading enzymes, Metabolic profiles.

Resumo

Cryphonectria parasitica, o agente causal do cancro do castanheiro, provoca lesões necróticas (cancros) na casca do tronco e ramos de hospedeiros suscetíveis. O micovírus *Cryphonectria hipovírus* 1 (CHV1) infecta *C. parasitica* e reduz a virulência do fungo (hipovirulência) e altera a morfologia do fungo em cultura (capacidade de pigmentação e esporulação). Dadas essas características, o micovírus CHV1 é usado na Europa como

agente de controlo biológico para o tratamento do cancro do castanheiro. O objetivo deste trabalho é entender melhor o efeito do micovírus na patogenicidade do fungo, comparando a produção de algumas enzimas que degradam a lenhina entre estirpes virulentas e hipovirulentas (convertidas e originais), assim como os perfis metabólicos. Para a avaliação qualitativa, vários compostos diferentes foram utilizados como indicadores para a produção de enzimas lenhinolíticas. Para a avaliação quantitativa, foram escolhidas cinco estirpes para testes biológicos e cultura em-meio líquido mínimo, e a quantidade de enzima produzida analisada. Verificou-se que estirpes virulentas causam maior dimensão da lesãonos ramos do castanheiro e produzem mais enzimas lenhinolíticas. Em maças, algumas das estirpes hipovirulentas produziram lesões maiores do que as de tipo selvagem. Paralelamente, foram usadas pela primeira vez microplacas Biolog FF com estirpes de *C. parasitica,* para avaliar perfis metabólicos com leituras simultâneas de 95 fontes de carbono diferentes. Hidratos de carbono, aminoácidos, aminas / amidas, compostos diversos e polímeros foram mais consumidos pelas estirpes hipovirulentas; o que pode sugerir um mecanismo de adaptação ecológica do fungo.

Palavras-chave : *Cryphonectria parasitica*, cancro do castanheiro, hipovirulência, enzimas degradadoras de lenhina, perfis metabólicos

Dedication

There are a number of people without whom this thesis might not have been written, and to whom I am greatly indebted.

To my mother and father who continue to learn, grow and develop and who have been a source of encouragement and inspiration to me throughout my life. May almighty God keep you and give your health.

To my sister, brother and friends who knowingly and unknowingly led me to an understanding of some of the more subtle challenges to our ability to thrive.

Acknowledgement

Table of contents

List of figures

List of tables

Abbreviations

ABTS - Diammonium salt 2,2′-azino-bis

AWCD - Average well color development

ICL - Isocitrate lyase

Lac - Laccase

LiP - Lignin peroxidase

MnP - Manganese peroxidase

OAH - Oxaloacetate acetylhydrolase

PEPM - Phosphoenolpyruvate mutase

VCG – vegetative compatibility group

I. Introduction

The chestnut is one of the most useful trees in the temperate regions considering the importance of chestnuts as a high carbohydrate food source and timber producer. In the world there are 4 major species: American Chestnut (*Castanea dentata*), European Chestnut (*C. sativa*), Chinese Chestnut (*C. mollissima*) and Japanese Chestnut (*C. crenata*) (Rigling and Prospero, 2017). Chestnut trees can be attacked by lethal diseases such as Chestnut Blight (*Cryphonectria parasitica*) and Ink Disease (*Phytophthora cinnamomi and Phytophthora cambivora*) (*Curculio elephas*), the chestnut moth *(Cydia splendana)* and the oriental chestnut gall wasp (*Dryocosmus kuriphilus*) (Santos, 2017). *Cryphonectria parasitica* is an Ascomycete fungus, it hosts mostly species in the genus *Castanea* causing chestnut blight, a devastating disease that create a great damage of the chestnut stands all over the world, but it can also infect oaks (*Quercus* spp.) and maples (*Acer* spp.). It is native to Eastern Asia and then accidently introduced into North America and Europe through infected chestnut plants (Rigling and Prospero, 2017). It was first detected in 1904 on American chestnut and caused the destruction of all chestnut trees on 4 million hectares in the beginning of this century (Smith, 2013). In the middle of the 20th century, it was introduced into Europe and destroyed most chestnut population in west-European countries (Smith, 2013).

In 1950, Biraghi noticed superficial (recovered) cankers on some chestnut trunks, and abnormal strains of the pathogen were isolated from naturally recovered cankers by Grente in 1964 (Tarcali, 2007). Lately, it was found that this pathogen can be infected naturally by a mycovirus called *Cryphonectria hypovirus* 1 (CHV1). This virus has the ability to control chestnut blight causing reduced parasitic growth, sporulation and pigmentation capacity and also diminishing the activity of pathogenesis–related enzymes, like oxaloacetate acethylhydrolase (OAH) (Chen *et al.*, 2010) and laccase (Chung *et al.*, 2008).

The aim of this project is to better understand the effect of the mycovirus on the fungi by comparing the production of some lignin degrading enzymes and the metabolic profiles of some virulent and hypovirulent (converted and original) strains. For qualitative evaluation, several different compounds have been used as indicators for ligninolytic enzymes production. For quantitative evaluation, among nine strains five were chosen for

biological tests and cultivation in minimal liquid media and the amount of laccase, lignin peroxidase and manganese peroxidase produced were analyzed. The Biolog FF MicroPlate system (Biolog Inc.) was used to characterize filamentous fungi according to their metabolic profiles. These profiles were obtained from fungus utilization of 95 carbon sources from different chemical groups (amines/amides, amino acids, carbohydrates, carboxylic acids, polymers and miscellaneous compounds). This method has been used to identify and aid the definition of new species of fungi with small morphological variation, when molecular techniques are of limited application (Rice and Currah, 2005). Biolog FF MicroPlates was used with *C. parasitica* to assess their metabolic profiles and functional diversity.

II. Literature review

This literature review contains information about strains of *Cryphonectria parasitica*, Chestnut Blight, its symptoms and artificial and natural control of this disease. It also provides information about lignin degrading enzymes.

1. Cryphonectria parasitica

1.1 Taxonomy

Cryphonectria parasitica (Murr.) Barr. is a Sordariomycete (Ascomycete) fungus in the family *Cryphonectriaceae* (Order Diaporthales). Closely related species that can also be found on chestnut include *C. radicalis*, *C. naterciae* and *C. japonica.*

1.2 Host range

C. parasitica hosts are particularly species that belong to the genus *Castanea* in the family Fagaceae: the American chestnut (*C. dentata*), the European chestnut (*C. sativa*), the Chinese chestnut (*C. mollissima* Blume) and the Japanese chestnut (*C. crenata* Siebold & Zucc.) (Rouan *et al.*, 1986). *Cryphonectria parasitica* can also attack other species such as oaks (*Quercus* spp.), post oak (*Q. stellata* Wangenh.), scarlet oak (*Q. coccinea* Münchh.), live oak (*Q. virginiana* Mill.) and white oak (*Q. alba* L.) in the USA, and holm oak (*Q. ilex* L.), sessile oak [*Q. petraea* (Mattuschka) Lieblein], downy oak (*Q. pubescens* Willd.) and Hungarian oak (*Q. frainetto* Ten.) in Europe (Rigling and Prospero, 2017). Occasionally, *C. parasitica* has also been found on maples (*Acer* spp.), European hornbeam (*Carpinus betulus* L.) and American chinkapin (*Castanea pumila* L. var. *pumila* and *C. pumila* var. *ozarkensis*) (Rigling and Prospero, 2017).

1.3 Life cycle and reproduction

C. parasitica enter to the host bark through fresh formed wounds or crack in the bark (Rouane *et al*., 1986).

Both asexual and sexual spores are able of causing infection (Prospero *et al.*, 2006), these spores are produced in the stroma, which holds a perithecium or a pycnidium: perithecium where the sexual ascospores are produced, pycnidium where the asexual conidia are produced. These spores are released from the stroma and spread on the infected bark (Smith, 2013).

The type of reproduction is determined by environmental factors like the nutrition available, temperature, and light (Smith, 2013). Sexual reproduction can be induced by

nitrogen starvation, light, and low temperatures (Smith, 2013). In *C. parasitica*, mating is controlled by a single mating type (MAT) locus, which contains either the MAT-1 or MAT-2 allele (Marra *et al.*, 2004). A conidium (with one mating type) acts as a male gameta, fertilizes a receptive hypha of the other mating type. *C. parasitica* has also a mixed mating system, with outcrossing and self-fertilization occurring at variable frequencies (Marra *et al.*, 2004).

These conidia are formed by mitosis and are genetically identical to the mycelium. They are generally dispersed to nearby trees by carriers such as insects and birds as well as rain (Rigling and Prospero, 2017).

Sexual and asexual fruiting bodies develop in masses of yellow–orange to red–brown pustules named stromata (Figure 1) and degrade the tissues down to the cambial layer of the tree. The cambial layer is essential for production of the xylem and phloem. Once a tree branch has become girdled, an important reduction in the transport of water and nutrient is observed (Rigling and Prospero, 2017).
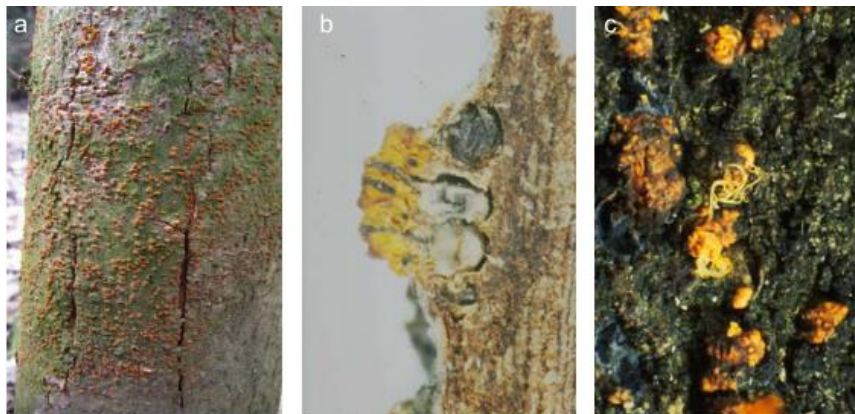
Figure 1 - Sporulation of *Cryphonectria parasitica*. (a) On the infected bark, the fungus produces masses of yellow–orange to reddish– brown pustules (stromata) harbouring sexual or asexual fruiting bodies. (b) Sexual fruiting bodies (perithecia). (c) Asexual fruiting bodies (pycnidia). The asexual spores (conidia) are extruded from the pycnidia as spore tendrils (adapted from Rigling and Prospero, 2017).

1.4 Vegetative compatibility

What is interesting in *C. parasitica* is that its vegetative incompatibility system restricts the horizontal transmission of virulence-attenuating mycoviruses between fungal individuals (Anagnostakis, 1977). To date, six unlinked vegetative incompatibility (vic) loci, each with two alleles, have been identified (Cortesi and Milgroom, 1998). These six di-allelic vic loci define 26564 vic genotypes, which correspond to 64 different vc types

(Biella *et al*., 2001). Two isolates are vegetative compatible if they have the same alleles at the six vic loci, so a co-culture of this two isolates on the same agar plate will combine into a single culture, otherwise if the isolates are vegetative incompatible, a barrage line will be formed along the contact zone (Figure 2), as a result of a programmed cell death (apoptosis) (Biella *et al*., 2002).
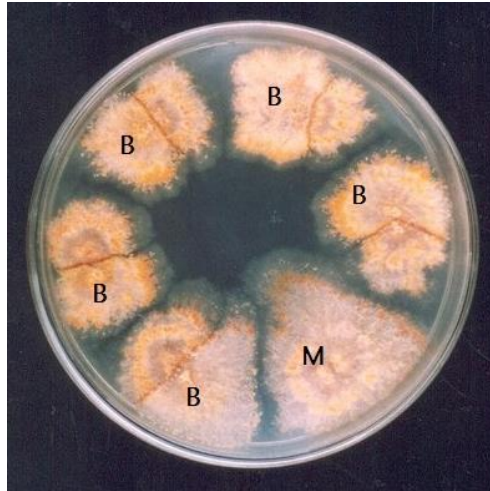
Figure 2 - (B)Vegetative incompatibility and (M) Vegetative compatibility.

1.5 vc-types distribution

Less vc types were found in Germany and Macedonia due to a recent introduction of the disease in these areas and/or low vic-allele diversity, in the other hand, more vc-types have been observed in areas, where the disease has been introduced from a long time and where sexual reproduction is more frequent e.g. France, Italy and Switzerland (Onofre *et al*., 2007).

Some vc-types are frequent in areas but rare in others, like a geographic distribution pattern. For example, EU-12 is the dominant vc type in southern Italy, Greece and eastern Europe, whereas EU-1, EU-2 and EU-5 are dominant in northern Italy, southern France, Switzerland and eastern Spain (Robin and Heiniger, 2001).

In Portugal, Trás-os-Montes is the most important chestnut-growing province with 85% of the total area of chestnut orchards and 79% of chestnut forests (INE, 2004). In the recent years, the disease has spread from the initial foci to other areas (Bragança *et al*., 2005) and the most dominant vc type in Portugal is EU-11, which represents 80.2% of all isolates, but other vc types have been found such as EU-28 and P-9 (Onofre *et al*., 2007).

2. Chestnut blight

2.1 Invasion history

During the 20th century the pathogen was introduced into north America and Europe (Griffin, 1986) through infected chestnut plants coming from Japan (Myburg *et al.*, 2004). After its first detection in 1904 in New York, the pathogen spread at a rate of more than 30 km per year (Anagnostakis, 1977) causing severe ecological and economic problems (Elliott and Swank, 2008). In Europe, it was first detected in 1938 in Italy, near Genoa (Ringling and Prospero, 2017). By 1950, the disease spread into France, Switzerland and Slovenia and then into eastern and south-eastern Europe and Turkey (Rigling and Prospero, 2017). A different genetic lineages of *C. parasitica* have been found in south-western giving the idea of an additional introduction into south Europe (Dutech *et al.*, 2009).

2.2. Disease symptoms

The manifestation of symptoms depends on the virulence of the strain of *C. parasitica* and the age of the infected tree part. Necrotic lesions are formed by virulent strains of *C. parasitica*, these lesions are capable of causing mortality to small branches (Figure. 3a, b, c, d). On thicker branches or stems perennial cankers are formed, this type of cankers may develop over years before killing the branches (Figure. 3a). Bark cankers on young stems/branches are orange to reddish-brown on the surface. On older stems/branches, canker coloration is generally less pronounced. *C. parasitica* develops a longitudinal splits and typical pale brown mycelial fans in the bark, the leaves wilt, turn yellow or brown (Figure. 3f). Trees react to an infection by producing numerous epicormic shoots below the cankers (Figure 3b) (Rigling and Prospero, 2017).

| a | b | c | d | f |
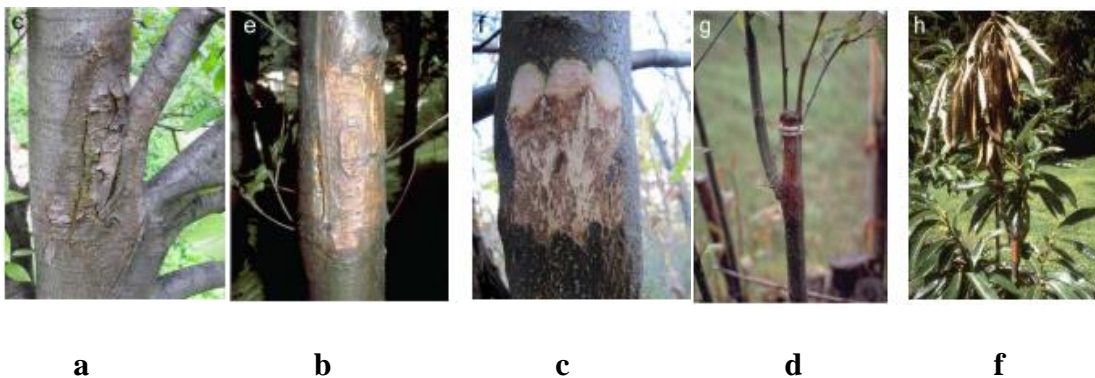
Figure 3- Symptoms of chestnut blight on *Castanea sativa* (adapted from Rigling and Prospero, 2017)

3. Factors related to the virulence of *C. parasitica*

After splitting the tree tissues and advancing in the bark, the chestnut tree tries to reform the wound caused by the pathogen, but it's inhibited by cell wall degrading enzymes and metabolites produced by *C. parasitica* such as oxalic acid, which has toxic effect on host cells and induce cell wall degradation (Rigling and Prospero, 2017). A knock out of the gene encoding for the oxalic acid producing enzyme confirms the role of this substance in pathogenesis (Chen *et al*., 2010), but there is other virulence factors including a G-protein signaling (Gao *et al*., 1996), an Ste12 transcription factor (Deng *et al*., 2007), a tannic acid-inducible laccase (Chung *et al*., 2008), a cyclophilin (Chen *et al*., 2010), a protein kinase 2 (CK2)-mediated signaling (Salamon *et al*., 2010) and an inhibitor (CpBir1) of apoptosis proteins (Gao *et al*., 2013).

4. Oxidative enzymes involved in degradation of cell-wall components

4.1 Composition of the plant cell wall

Cell walls of plants are composed of cellulose, hemicellulose and lignin:

- Cellulose, the major constituent of all plant material, is a linear biopolymer consisting of anhydroglucopyranose molecules (glucose) connected by β-1,4- glycosidic bonds. Coupling of adjacent cellulose chains via hydrogen bonds, hydrophobic interactions and Van der Waals forces results in the parallel alignment of crystalline structures known as microfibrils (Dashtban *et al*., 2010).

- Hemicelluloses are heterogeneous polymers of pentoses (including xylose and arabinose), hexoses (mainly mannose, less glucose and galactose) and sugar acids. The highly variable composition of hemicelluloses is dependent on its plant source (Badal, 2000).

- Lignin, a heterogeneous polymer of lignocellulosic residues. It generally contains three precursor aromatic alcohols including coniferyl alcohol, sinapyl and p-coumaryl (Wei *et al*., 2009). These precursors form the guaiacyl-(G), syringyl-(S) and p-hydroxyphenyl (H) subunits in the lignin molecule, respectively (Speranza *et al*., 2005). The subunits ratio, and so, the lignin composition varies between different plant groups. Oxidative coupling of these lignin aromatic alcohol monomers creates a complex structure in lignin which is highly recalcitrant to degradation (Wong, 2009).

By linking to both hemicelluloses and cellulose, lignin acts as a barrier to any solutions or enzymes and prevents penetration of lignocellulolytic enzymes to the interior lignocellulosic structure. Beside Basidiomycetes white-rot fungi, most microorganisms are not able to degrade lignin (Dashtban *et al*., 2010).

4.2 Oxidative enzymes

Some fungal species such as *C. parasitica* are capable of lignin, cellulose, and hemicellulose decomposition and transforming this components into carbon dioxide (Rivera-Hoyos *et al*., 2013) by production of laccases (Lac), lignin peroxidases (LiP) and manganese peroxidases (MnP). Although LiP is able to oxidize the non-phenolic part of lignin (which forms 80-90% of lignin composition) (Wang *et al*., 2008), some studies of the early stages of the fungal degradation of wood have shown that oxidative ligninolytic enzymes are too large to penetrate into the wood cell wall micropores (Srebotnik *et al*., 1988). Thus, it has been suggested that prior to the enzymatic attack, low-molecular weight diffusible reactive oxidative compounds must initiate changes to the lignin structure (Tanaka *et al*., 1999). Figure 4 summarizes the major steps of lignin degradation process.

Lac: laccase, LMS: laccase-mediator system, LiP: lignin peroxidase, MnP: manganese peroxidase, VP: versatile peroxidase, H_2O_2-GO: H_2O_2-generating oxidases, AAO: aryl-alcohol oxidase, GLOX: glyoxal oxidase, H_2O_2: hydrogen peroxide AAD: aryl-alcohol dehydrogenases, QR: quinone reductases and $^{\bullet}OH$: free hydroxyl radicals.
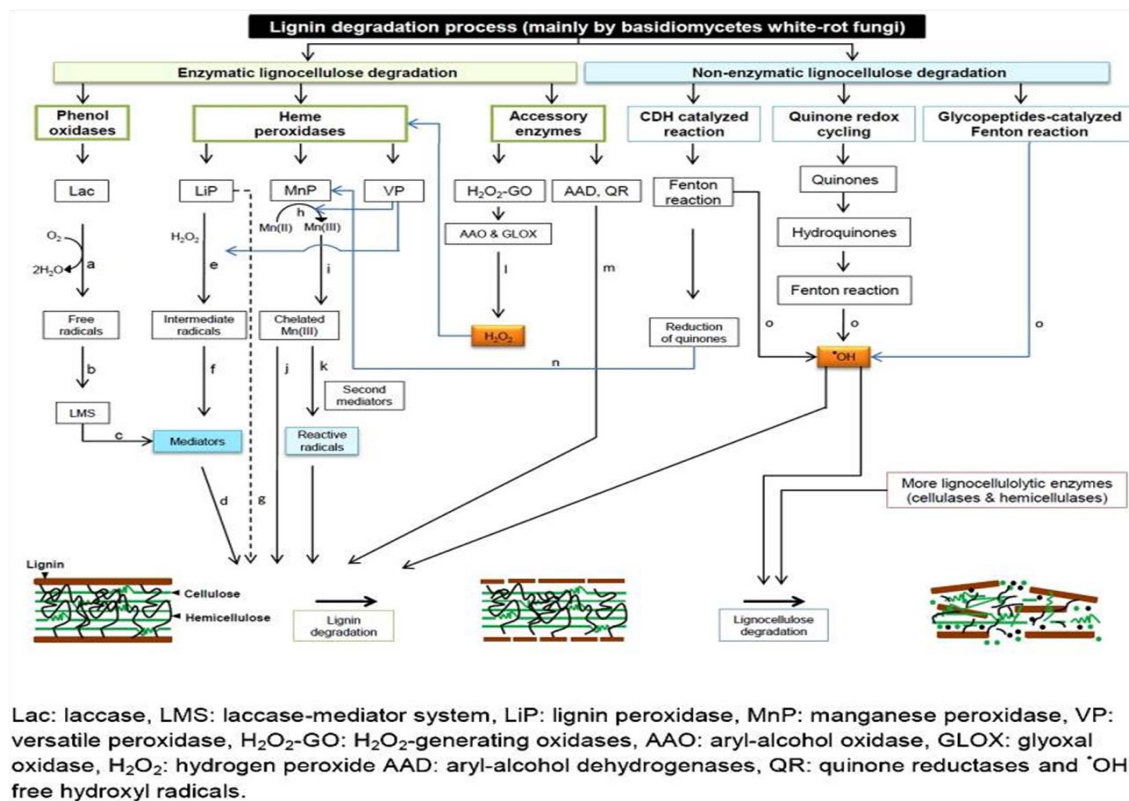
Figure 4 - Schematic diagram of lignin degradation by basidiomycetes white-rot fungi: the major steps and enzymes involved (adapted from Dashtban *et al*., 2010).

4.2.1 Oxaloacetate acetylhydrolase (OAH)

OAH (EC 3.7.1.1) is a member of the Phosphoenolpyruvate mutase (PEPM)/isocitrate lyase (ICL) superfamily. They take action on α-oxycarboxylate substrates to generate/divide C-C or P-C bonds. All PEPM/ICL superfamily members are oligomeric proteins, mostly tetramers, and each subunit adopts an $(\alpha/\beta)8$-barrel fold (Chen *et al.*, 2010). The active site could be found at the C-terminal side of the β-barrel. $Mg2+$ or $Mn2+$ are necessary for the activity of PEPM/ICL superfamily members, the metal mediates the interactions between the protein and the substrate (Chen e*t al.*, 2010). Oxaloacetate acetylhydrolase catalyzes the hydrolysis of oxaloacetate to oxalic acid and acetate (Figure 5). Oxalic acid production and secretion are related with fungal pathogenesis and virulence (Kirkland *et al.*, 2005) The virulence mechanism is caused by acidification that activates lignocellulose degradation, diminishes viability of host tissue in favor of pathogen proliferation, and induces crystallization of calcium oxalate, which blocks vessels (Nakagawa and Shimazu, 1999).
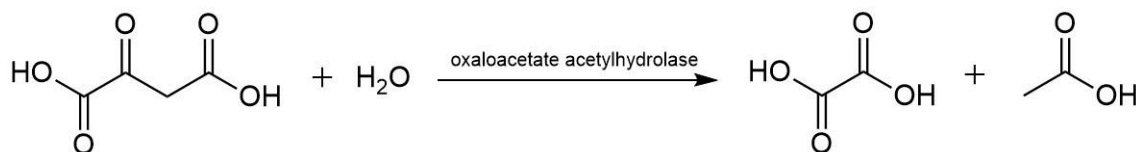
Figure 5 -The OAH-catalyzed reaction.

4.2.2 Laccase

Laccase (EC 1.10.3.2), p-diphenol oxidase (systematic name – benzenediol: oxygen oxidoreductase), was for the first time extracted from a plant in 1883 (Kaczmarek and Kwiatos, 2017). Actually, there are many identified laccases, either extracellular or intracellular. They are glycoproteins, which most frequently occur as isoenzymes, and by oligomerization of subunits, can form multimeric complexes, mainly dimeric or tetrameric with a mass that ranges from 50 kDa to 100 kDa (Thurston, 1994).

Laccases, popularly named as the blue oxidases, belong to the multicopper oxidases (MCOs) superfamily (Arora and Sharma, 2010) and they have the capacity to oxidize organic and inorganic compounds such as mono-, di, poly-, amino- and methoxyphenols, and a number of aromatic amines. The final step of the reactions of this oxidoreductases is the reduction of molecular oxygen to two water molecules, that's why laccases are viewed as "ideal green" catalysts (Galhaup and Haltrich, 2001).

Beside simple phenolic derivates, laccase can catalyze the oxidation of a wide range of substrates, by mediators interacting in the transport of electrons between the substrate and the catalytic center of the enzyme (Kersten *et al.*, 1990).

The most frequently applied synthetic mediators are diammonium salt 2,2'-azino-bis (3-ethylbenzothiazoline-6-sulfonic acid) (ABTS), hydroxybenzotriazole (HBT), hydroxyanthranilic acid (HAA), violuric acid, hydroxyyacetanilide (NHA) and hydroxyphthalimide (HPI). It has been proved that oxidation of veratryl alcohol to aldehyde is approximately 5-fold more efficient in the presence of ABTS as a mediator (Kaczmarek and Kwiatos, 2017). Fungal laccases are involved in sporulation, pigment production, fruit body formation, and plant pathogenesis (Rivera-Hoyos *et al.*, 2013).

4.2.3 Lignin peroxidase (LiP)

Lignin peroxidase, (EC 1.11.1.14) is a glycoprotein that contains a heme, cleaves C-C bonds and oxidizes benzyl alcohols to aldehydes or ketones. LiP is capable to catalyze both phenolic and non-phenolic lignin substructures by a one-electron oxidation reaction to generate unstable aryl radical cations. It's necessary to have an extracellular hydrogen peroxide, to act as an electron acceptor. LiP is capable of the initiation of different non-enzymatic reactions such as the cleavage of Cα-Cβ bond in the side chain, β-O-4 bond between side chain and next ring and cleavage of aromatic ring (Figure 6) (Swe, 2011).
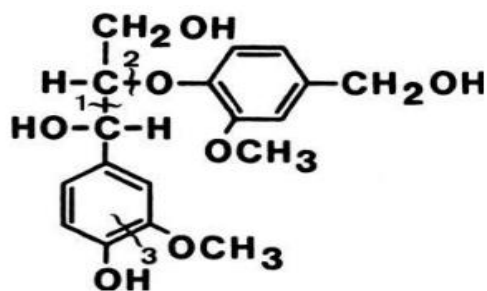
Figure 6 - Reactions initiated by lignin peroxidase: (1) cleavage of Cα-Cβ bond in the side chain, (2) β-O-4 bond between side chain and next ring and (3) cleavage of aromatic ring (adopted from Swe, 2011).

4.2.4 Manganese peroxidase (MnP)

Manganese peroxidase (EC 1.11.1.13), is a heme containing glycoprotein, attacks phenolic lignin components. Only some basidiomycetes and wood decaying white-rot fungi can produce this enzyme. It oxidizes Mn^{2+} to Mn^{3+} and H_2O_2 acts as an electron acceptor. The first step of the catalytic cycle of MnP is the binding of H_2O_2 to the native

ferric enzyme and the formation of iron-peroxide complex. The heme will provide two electrons for the cleavage of oxygen-oxygen bond of hydrogen peroxide to one water molecule, which generate the MnP Compound I (Fe4+-oxo-porphyrin-radical complex). By a monochelated Mn2+, this MnP Compound I is reduced to MnP Compound II (Fe4+-oxo-porphyrin complex), thus Mn3+ is formed. By the reduction of MnP Compound II by Mn2+ and the releasing of another water molecule the native enzyme is reformed. Then, a strong oxidant is generated, Mn3+, which oxidizes phenolic structures by single electron oxidation (Figure 7) (Swe, 2011).
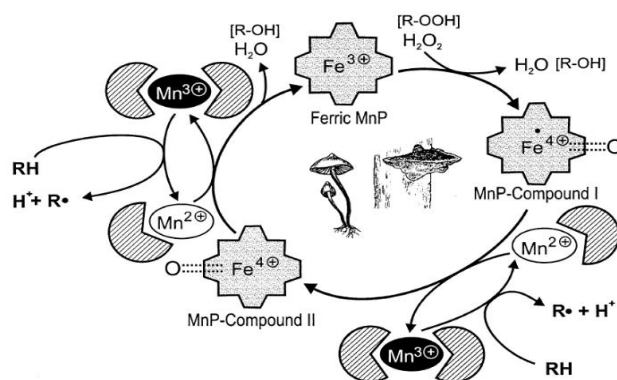
Figure 7 - Catalytic cycle initiated by Manganese Peroxidase (adapted from Swe, 2011).

4.2.5 Versatile peroxidases (VP)

Versatile peroxidases were first discovered in 1999 in members of the genus *Pleurotus* (Dashtban *et al*., 2010). They are glycoproteins with the ability to oxidize typical substrates of other peroxidases including Mn (II) and also veratryl alcohol (VA), MnP and the typical LiP substrate, respectively (Dashtban *et al*., 2010). Due to their hybrid structures, VPs can provide multiple binding sites for the substrates that's why they have the ability to oxidize Mn (II), phenolic and nonphenolic aromatic compounds (Wesenberg *et al*., 2003). This makes VPs more efficient than LiP and MnP, because they are not able to efficiently oxidize phenolic compounds in the absence of VA or oxidize phenols in the absence of Mn (II), respectively (Ruiz- Dueñas, 2009).

Table 1 - Features of the main two groups of fungal ligninolytic enzymes (adapted from Dashtban *et al.*, 2010)

Type of enzymes	Reaction[1]	Cofactor	Metals or ions[2]	Mediators	Subunits & molecular mass (kDa)	Range of optimum temperature (°C)	Range of pH optimum	Localization	Glycosylation
Phenol oxidase (laccase)	4 benzenediol + O_2 = 4 benzosemiquinone + 2 H_2O	N/A	Ca^{2+} Cd^{2+} Cu^{2+} H_2O_2 Imidazole K^+ K_2SO_4 Mn^{2+} Na_2SO_4 $(NH_4)_2SO_4$	Phenols, aniline, 3-HAA, NHA, syringaldehyde, hydroxybenzotri azole and ABTS	Monomeric (43-100), dimeric, trimeric & oligomeric (e.g. tetramers with ~390 KDa)	20-80	2-10	Mostly extracellular[3]	Yes (*N*-glycosylated)[4]
Peroxidases:	1,2-bis(3,4-dimethoxyphenyl)propane-1,3-diol + H_2O_2 = 3,4-								
a) Lignin peroxidase (LiP)	dimethoxybenzaldehyde + 1-(3,4-dimethoxyphenyl)ethane-1,2-diol + H_2O	Heme	Iron	Veratryl alcohol	Monomeric (37-50)	35-55	1-5	extracellular	Yes (*N*-glycosylated)[4]
b) Manganese peroxidase (MnP)	2Mn(II) + 2H^+ + H_2O_2 = 2Mn(III) + 2H_2O	Heme	Ca^{2+} Cd^{2+} Mn^{2+} Sm^{3+}	Organic acid as chelators, thiols, unsaturated fatty acids	Monomeric (32-62.5)	30-60	2.5-6.8	extracellular	Yes (*N*-glycosylated)[4]
c) Versatile peroxidase (VP)	donor + H_2O_2 = oxidized donor + 2H_2O (e.g. reactive black 5 + H_2O_2 = oxidized reactive black 5 + 2H_2O)	Heme	Mn^{2+} Ca^{2+} Cu^{2+} Iron	Veratryl alcohol, compounds similar to LiP and MnP mediators	Monomeric	Not known	3-5	extracellular	Yes

5. Management of the disease

5.1 Quarantine measures for control of the disease

To reduce the movement and spread of *C. parasitica* some quarantine regulations have been adopted, so chestnut and oak plantlets can only be moved within Europe if they are accompanied by a plant passport which certifies that: (i) the plants came from areas free from *C. parasitica*; or (ii) no observation of *C. parasitica* has been made at the production place or its immediate vicinity since the beginning of the last complete cycle of vegetation, nevertheless these regulations were ineffective to completely stop the spread of the pathogen because the infection wasn't always detectable by visual examination (Rigling and Prospero, 2017).

Cutting and burning of the infected plants wasn't successful too because it's difficult to find all the inoculum sources (Prospero and Rigling, 2013).

Avoiding wounds in the bark may be a successful way to reduce the spread of the disease and when wounds are unavoidable (pruning or grafting), the wounding shouldn't be done in the period of spore production (Rigling and Prospero, 2017). Chemicals are not an option because of the restriction of its use in some forests, and some fungicides have proven to be phytotoxic (Trapiello *et al.*, 2015).

5.2 Natural control of the disease: *Cryphonectria hypovirus* 1 (CHV1)

Hypovirus that infect *C. parasitica* are double-stranded RNA (dsRNA) viruses without a coat protein, incorporated with fungal membrane vesicles and located in the cytoplasm. There have been identified four species, namely *Cryphonectria hypovirus* 1 (CHV1), CHV2, CHV3 and CHV4. The one that causes hypovirulence to *C. parasitica* and acts as biological control agent of chestnut blight in Europe is CHV1, which decreases the parasitic growth and sporulation capacity of the pathogen (Rigling and Prospero, 2017). There are subtypes of CHV1 with different levels of virulence, some reveal severe symptoms in *C. parasitica* and decrease almost completely the sporulation (e.g., CHV-1/EP713), and other are milder and concede more sporulation, (e.g., CHV1/Euro7). This mild strains of CHV1 are much more frequent in Europe (Milgroom and Cortesi, 2004). CHV2, CHV3 and CHV4, are taxonomically related to CHV1, but they are different from CHV1 by the genome organization and the effect on *C. parasitica* (Hillman and Suzuki, 2004). While CHV2 and CHV3 can cause hypovirulence to *C. parasitica*, CHV4 causes no significant symptoms in its fungal host (Rigling and Prospero, 2017).

The spread of this hypovirus depends on the combination of horizontal transmission (to other fungal individuals) and vertical transmission (to spores) of the hypovirus. From a hypovirus-infected fungal individual, the hypovirus is only transmitted into asexual spores (conidia), but not into sexual ascospores (Prospero *et al.*, 2006). It is dispersed with the conidia and then transmitted from the outgrowing spores to other fungal individuals via hyphal anastomosis (Milgroom and Cortesi, 2004).

The hypovirus transmission is limited by the vegetative incompatibility of *C. parasitica* strains. To know the ability of transmission between two strains, a co-culturing pairs of hypovirus- infected and hypovirus-free strains on potato dextrose agar (PDA) plates is performed and the change of the orange morphology of hypovirus-free strains to a white morphology of the hypovirus-infected strains enables the visual evaluation of hypovirus transmission (Rigling and Prospero, 2017).

Some studies have revealed that some *C. parasitica* proteins are down-regulated in the presence of CHV-1 such as laccase, oxaloacetate acetylhydrolase (Chen *et al.*, 2010), pheromone-encoding gene, cryparin: a cell wall hydrophobin (Turina and Rostagno, 2007), some gene are shown to be disrupted, e.g. CpMK1 (is a Hog 1 homologue from *C. parasitica*, related to pigmentation, conidiation, laccase production and cryparin expression) (Park *et al.*, 2004), also cpg-1 (one of G-protein components, which is required for efficient hyphal growth, orange pigmentation, conidiation and sexual reproduction) (Turina and Rostagno, 2007).

6. Objectives

1. Convert virulent strains (EU-11, EU-66) to hypovirulent by the CHV-1 hypovirus (RB111).

2. Evaluate the degree of virulence of the virulent and hypovirulent strains of *C. parasitica.*

3. Evaluate the production of laccase, lignin peroxidase and manganese peroxidase in virulent and hypovirulent strains of *C. parasitica*

4. Evaluate the differences in metabolic profile of virulent and hypovirulent strains of *C. parasitica.*

III. Materials and Methods

1. Characterization of *Cryphonectria parasitica* isolates

1.1 *Cryphonectria parasitica* isolates

C. parasitica isolates used in this study, listed in Table 2, were obtained from different locations in chestnut plantation field. These strains were re-cultured and maintained, on Potato Dextrose Agar (PDA, 39g/L) after sterilization at 120°C for 20min.

Table 2 – Strains information of *C. parasitica* isolates

Date	Code	VCG	Sites	Virulence
2018	Cast13	EU11	Castrelos (Bragança)	Virulent
2018	Cast26	EU11	Castrelos (Bragança)	Virulent
2018	VBC02	EU11	Vila Boa Carção (Bragança)	Virulent
2011	RB111	EU11	Rio Bom (Valpaços)	Hypovirulent
2017	Serra05	EU11	Serra (Chaves)	Hypovirulent
2013	SR442	EU11	Sergude (Felgueiras)	Hypovirulent
2018	Cast07	EU66	Castrelos (Bragança)	Virulent
2018	Cast17	EU66	Castrelos (Bragança)	Virulent
2014	VDP11	EU66	Vilar de Peregrinos (Vinhais)	Virulent

1.2 Conversion of virulent strains

Conversions were made by placing virulent (Cast13, VBC02, Cast26) and hypovirulent (RB111) isolates of *C. parasitica* approximately 5mm apart at the edge of a Petri dish containing PDA. Mycelium of the converted strains were removed and transferred to fresh PDA medium.

1.3 Evaluation of the virulence of *C. parasitica* isolates by inoculation in apples

For this assay we used five isolates of *C. parasitica* with at least seven days of growth and apples homogenous and without defects or decay and finally washed in distilled water and dry.

A sterilized Pasteur glass pipette was used to obtain circular mycelial sections of *C. parasitica* isolates for the use as an inoculum, as shown in Figure 8. With another sterilized Pasteur glass pipette, holes were made in the apples as shown in the Figure 9.

Figure 8 - Drilling holes in *C. parasitica.*

Figure 9 - Drilling holes in the apples.

With the help of a tweezers *C. parasitica* inoculum was placed into the apples (with three replicates for each isolate), and it was sealed with parafilm (Figures 10 and 11). Each of the replicates was identified and apples incubated at 24ºC in the dark for seven days.

Figure 10 - Covering the inoculum with parafilm.

Figure 11 - Inoculated apples in incubation tray.

Presence of lesions and their growth [largest radius (r>) and minor radius (r <)] were evaluated in mm after seven days incubation time, as shown in Figure 12.
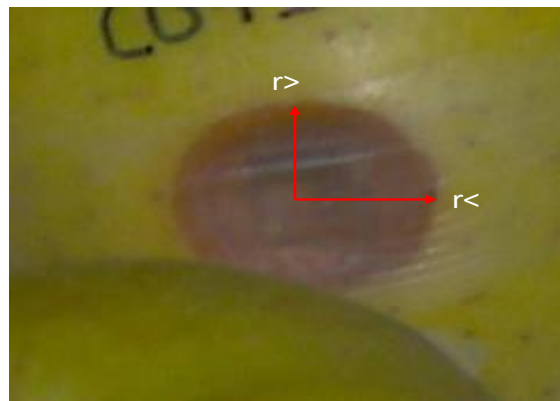
Figure 12 - Rot lesion in an apple.

1.4 Evaluation of the virulence of *C. parasitica* isolates in young branches of *Castanea sativa* Mill.

Chestnut branches were collected in *C. sativa* nurseries at ESAB-IPB open fields.

Figure 13 - Young chestnut tree.

Chestnut branches were cut into sections approximately 20 cm long. Wax was applied on both cutting sides of the branches to avoid desiccation of the wood, as shown in Figure 14 and 15.

Figure 14 - Chestnut branches.

Figure 15 - Wax application.

It was used a scalpel to do a cut in the middle of each branch, and a Pasteur glass pipette to obtain mycelia from each isolate from a Petri plate. Then, inoculations of the three hypovirulent and two virulent strains of *Cryphonectria parasitica* at the cut site were made using a loop. The name of the isolate was registered in the branch. The all steps in the process can be visualized in Figures 16 and 17.

Figure 16 – Cutting the branches.

Figure 17 - Application of inoculum.

After inoculation, the inoculation sites were covered with cotton wool moistened with distilled water and surrounded with parafilm to avoid loss of moisture (Figure 18).

Figure 18 - Cover with cotton and parafilm.

Finally, chestnut branches were placed on a laboratory tray in an incubation chamber at 25ºC in the light. They were checked for fungal growth after six days. If there was any, registration and measurement of the growth were made. Disease growth was checked in two directions (r1(cm), r2(cm)) from the center.

1.5 CHV1 virus detection protocol

1.5.1 RNA Extraction and CHV1 identification

The presence of CHV1 (*Cryphonectria hypovirus* 1) was verified through the presence of double-stranded RNA (dsRNA). For the extraction of dsRNA, the isolates that presented morphological characteristics of hypovirulence were grown in Petri dishes with PDA medium for seven days at 25 ºC in the dark. The mycelium was removed and macerated using liquid nitrogen. Total RNA was isolated from mycelium using the NorGen BioTek kit (Thorold, ON, Canada). Extraction was done using lysis buffer, precipitated with 100% ethanol and washed in columns with wash solution. The RNA was dissolved in elution buffer and stored at -20°C.

The ORF-A region was amplified using the primers hvep-1F (5`-TGACACGGAAGCTGAGTGTC-3´) and EP-721-4 (5´-

GGAAGTCGGACATGCCCTG - 3´). For the ORF-B region were utilized the primers orfB-12aF (5´- AGACCTCAATCGGGTCTCCCT - 3´) and orfB-12aR (5´- TTCAACCACACGACGAGTTCG - 3´). PCR amplification was performed using 1 µl of cDNA in a total of 50 µl reaction volume consisted of 10 µl of 2X Jump Start (Sigma) and 1 µl of each primer (20 pmol/µl). Thermocycling conditions were set up with an initial denaturation at 94 °C for 2 min, followed by 33 cycles consisting of 94 ºC denaturation for 1 min, annealing at 55 °C for 1,5 min, and elongation at 72 °C for 2 min, with a final extension at 72 ° C for 8 min. The PCR products were visualized by agarose gel electrophoresis on 1.5% gel stained with GelRed® Nucleic Acid Gel Stain (Biotium, Inc) under UV illumination.

2. Qualitative and quantitative evaluation of ligninolytic enzyme production

2.1 Qualitative enzymatic assays

Nine strains were used for the qualitative evaluation: six virulent strains (3 EU11, 3 EU66) and 3 hypovirulent strains.

2.1.1 Bavendamm test (phenol oxidase test)

The medium contained 1.5% malt extract, 1.5% agar and 0.5% tannic acid, pH=4.5. The solution with tannic acid was prepared, autoclaved separately and mixed with the other components before pouring into Petri dishes. Petri plates were inoculated with plugs from fungal strains catted with glass Pasteur pipettes. Incubation at 25°C in darkness.

2.1.2 Peroxidases medium

For peroxidases evaluation it was used PDA with 25mg/l Azur B added. After sterilization it was aseptically transferred into rectangular Petri dishes, inoculated and Incubated at 25°C in darkness.

2.1.3 Cellulase medium

The medium was prepared with 0.5% of carboxymethyl cellulose (CMC) and 1.6% agar for the growing of nine isolates. Four days after inoculation and incubation at 25°C, the plates were flooded with a 0.1% solution of Congo Red for 45min, then the stain was poured off, and they were destained with a 1M solution of NaCl for 15min. An uninoculated plate was used as a control for media decolorization.

2.1.4 Screening for laccase and peroxidases

It was used malt extract agar (MEA) medium supplemented with 0.04% RBBR and 200µM $CuSO_4$. For this, solutions of 20% of RBBR and 400mM of $CuSO_4$ were prepared and filtered through a 0.2µm filter. As controls two uninoculated plates were used: one with the dye (as abiotic control) and one without dye (as biotic control).

2.2 Quantitative enzymatic assays

2.2.1 Media and cultures conditions for enzymes quantification

For quantitative enzymatic assays five strains were selected: two virulent (Cast13 and VBC02), their converted ones (Cast13c and VBC02c) and one hypovirulent strain (RB111). These strains were incubated for four days in a sterile PDB medium in 250ml Erlenmeyer flasks and incubated at 110rpm, at 25°C. Then, the mycelium was filtered and transferred to a minimal medium with 62.5ml salt solution, 2mg thiamine, 10g glucose in a 1liter.

Salt solution contained: 24g/l NH_4NO_3, 16g/l KH_2PO_4, 4g/l Na_2SO_4, 8g/l KCl, 2g/l $MgSO_4 \cdot 7H_2O$, 1g/l $CaCl_2$, 8ml/l of a trace elements solution. Trace elements solution is composed of: 60mg/l H_3BO_3, 140mg/l $MnCl_2 \cdot 4H_2O$, 400mg/ml Z_nCl_2, 40mg/l Na_2MoO_4, 100mg/l $FeCl_3 \cdot 6H_2O$, 400mg/l $CuSO_4 \cdot 5H_2O$.

The minimal medium was buffered at pH value 4, using a Na_2HPO_4 (0.2M)- citrate (0.1M) buffer. The Erlenmeyer flasks of 500ml, filled with 200ml minimal medium were autoclaved in 121°C for 20min and incubated at 110rpm, at 25°C. After 3 days of incubation the mycelium were filtered, freezed using liquid nitrogen and stocked at -80°C for molecular methods, the supernatant was centrifuged at 3200 rpm for 40 min and putted in tubes and stocked at -80°C for further analyses.

Note: Two similar culture medium were done following the previous method.

2.2.2 Enzyme assays

<u>Laccase activity</u> is determined by monitoring the oxidation of ABTS in citrate phosphate buffer, pH 3.6. The reaction mixture contains 0.2 mM of ABTS (555µl) and 250 µl of culture supernatant in a total volume of 5 ml. The oxidation of ABTS was measured by an increase in absorbance at 405nm. In the blank the supernatant was replaced by buffer. Laccase enzyme activity is further measured in units, one unit of enzyme activity (U) is defined as the amount of enzyme that released 1 µmole per minute of oxidized product.

<u>Lignin peroxidase (LiP)</u> activity is determined by monitoring the oxidation of azure B dye. The reaction mixture contained 1 ml of 125 mM sodium tartrate buffer (pH 3.0), 500

µl of 0.160 mM azure B, 500 µl of the culture filtrate and 500 µl of 2 mM H_2O_2. The reaction was initiated by adding peroxide hydrogen and the absorbance of each sample was taken at 651 nm after 5 min interval. One unit of enzyme activity has been expressed as an O.D. decrease of 0.1 units per minute per ml of the culture filtrate (Arora and Gill 2001).

The activity of <u>manganese peroxidase (MnP)</u> can be measured by the assay, which was performed by the addition of 0.4 mL $MnSO_4$ (1mM) in 1 mL sodium tartrate buffer (50mM) (pH 3.0) in the presence of 0.4 mL H_2O_2 (0.1mM) and 0.2 mL culture supernatant. Manganic ions Mn^{3+} form a complex with tartrate, the absorbance of each sample was taken at 270 nm after 5 min interval. One unit of Manganese peroxidase activity corresponds to the change in absorbance per minute at 25 °C.

Note: For the blank in Lignin and Manganese peroxidase assays, each sample, just after adding the hydrogen peroxide, was considered zero.

2.2.3 Total protein concentration

Total protein concentration was determined by Bradford Assay based on Bradford method with bovine serum albumin (BSA) as standard. the samples were containing between 10 and 100 µl in a total volume of 100 µl into glass tubes and 1mL of protein reagent then they were mixed gently. The absorbance was measured at 595 nm. The assay reagent was made by dissolving 100 mg of Coomassie Blue G250 in 50 mL of 95% ethanol. The solution was then mixed with 100 mL of 85% phosphoric acid and made up to 1 L with distilled water. The reagent was filtered and then stored in an amber bottle at room temperature.

Note: Quartz (silica) spectrophotometer cuvettes should not be used, as the dye binds to this material. Plastic and glassware used in the assay should be absolutely clean and detergent free.

3. Characterization of the metabolic profiles

3.1 Testing the viability of the mycelium used

Two virulent (Cast13 and VBC02) isolates, their converted ones (Cast13c and VBC02c) and one hypovirulent strain (RB111) were grown in 250ml Erlenmeyer with 100ml of PDB, using five plugs of each isolate. Four days of incubation time at 110 rpm, at 25°C. In each case, the mycelium was filtered and transferred to glass bottles.

Its viability was tested by counting the number of sections in a bottle with smashed mycelium (the smashing was done with a laboratory mixer). 10 µl of smashed mycelium were placed in a petri dish containing PDA and were spread throughout the plate (Figure

21), then the plates were incubated at 25°C in the dark for five days. The number of sections per plate were counted and per mL were calculated.
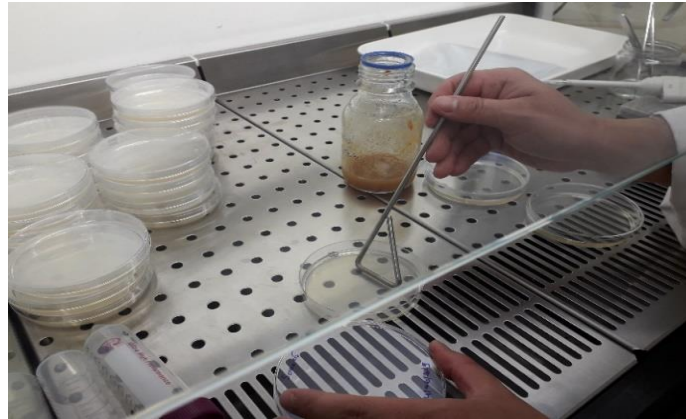
Figure 19 - Spreading the mycelium throughout the plate.

3.2 BIOLOG FF Microplates

The global phenotypes and utilization of 95 low molecular weight carbon sources (plus a negative control) by each of the isolates were evaluated using the Biolog FF Microplate (Biolog Inc.), following manufacturer instructions. The obtained mycelium (viable and non-contaminated) was suspended in FF inoculating fluid supplied by Biolog in glass tubes (Cat. Nº 1006), mixed gently by hand and adjusted to approx. 75 % transmittance at 590 nm using a Biolog Turbidimeter, previously calibrated using an FF Biolog Turbidity standard (Cat. Nº 3426) (Figure 19, 20). Smashed mycelium (100 µl) was added to each well, and the FF MicroPlates were then incubated at 25°C in the dark. The optical density at 490 nm (mitochondrial activity) was determined using an ASYS UVM 340 microplate reader (Hitech GmbH) for each plate at 24 h intervals over the next seven days. Carbon sources were considered not utilized in wells in which color development was less than, or equal to, that of negative controls.
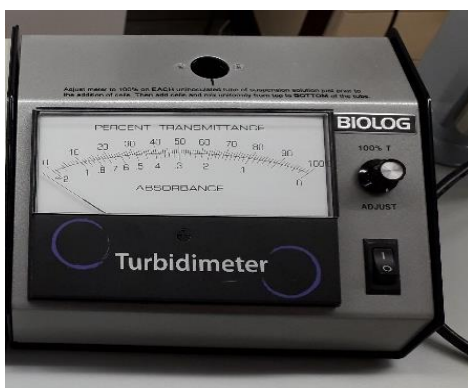
Figure 20 - BIOLOG Turbidimeter

Figure 21 - ASYS UVM 340 microplate reader

4. Statistical analyses

Multivariate analyses were performed in PAST v.3.18 to reduce the number of variables resulting from metabolic (Biolog-carbon source utilization) profiles, using Principal Component Analysis (PCA). For the metabolic profiles, the average well color development (AWCD) of the different replicates were calculated seven days after incubation, where AWCD equals the sum of the difference between the OD of the blank well (control) and substrate wells, divided by 95 (the number of substrate wells in the FF Microplate). The AWCD values were stabilized only at seven days, therefore OD readings obtained in each of the 95 carbon sources at this incubation time were then reduced to a smaller, easily interpretable, number of explanatory variables with PCA. Significant differences between the strains were calculated using Anova one way.

IV. Results

1. Characterization of *Cryphonectria parasitica* isolates

1.1 Conversion of virulent isolates to hypovirulent

The results of pairing between each of the three virulent strains: VBC02, Cast26 and Cast13 with the hypovirulent RB111, are shown in Figure 22.

Figure 22 - Conversion of three virulent strainsVBC02, Cast26 and Cast13.

The pairings show no separation lines between the two isolates (Figure 22). Single growth on PDA shows different morphologic characteristic than those from virulent isolates. Then, two chosen virulent strains, their converted ones and the hypovirulent were further tested for Pathogenicity and the presence of dsRNA (Figure 28). These isolates seem to be converted with visual observation but we need confirmation by biomolecular methods.

Figure 23 – Differences between virulent and hypovirulent strains of *C. parasitica* in the colony morphology, nine days post inoculation.

On PDA medium as we compared virulent strains with hypovirulent ones, RB111, Cast13c and VBC02c infected with CHV1 showed slow growth rate with an average of 6 mm per day, white mycelium color and no spores production, in the other hand, virulent

strains Cast 13 and VBC02 show high growth rate with an average of 10 mm per day, orange mycelium color, sectored colony margins and spores' production (Figure 23).

1.2 Pathogenecity tests

The results of inoculating five strains of *C. parasitica* in apple fruits and in chestnut branches are shown in Figures 24 and 25, respectively.

Figure 24 - Wounds of inoculated apples with *Cryphonectria parasitica* plugs, 10 days after inoculation.
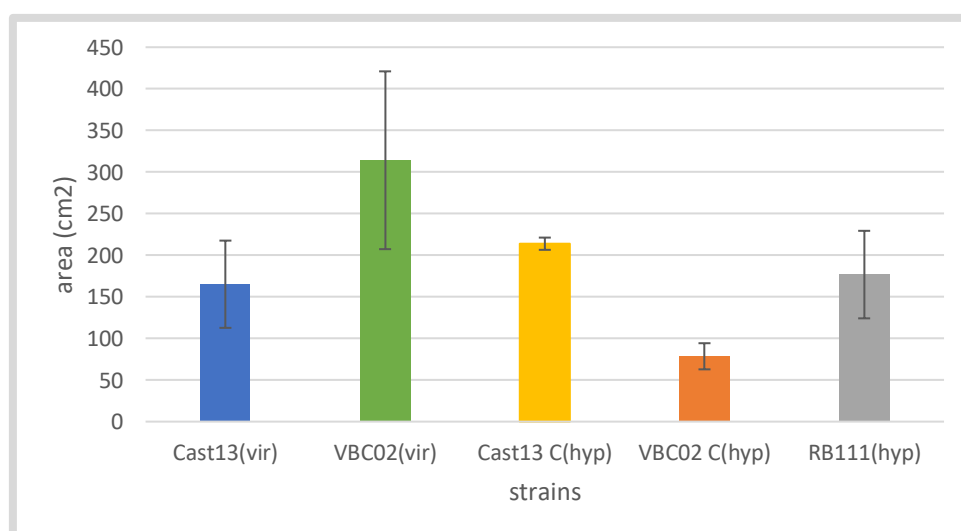
Figure 25 - Mean infection area caused by virulent and hypovirulent strains of *Cryphonectria parasitica.* 10 days after inoculation.

Apple fruit rot lesion measurements are presented in Appendix III. Infection area caused by VBC02 is higher than the one caused by its converted one (VBC02c), but the pattern between Cast13 and Cast13c are not similar, as shown in Figure 25. The infection area of the hypovirulent RB111 is even higher than that from Cast13, so infection areas may not be the only factor related with *C. parasitica* pathogenicity in *C. sativa.* p value = 0.009<0.05, results are significantly different (Appendix VI, Figure 45).

Chestnut lesion measurements are shown in Appendix IV. Hypovirulent strains caused small disease lesions but virulent strains caused large brown cankers on the shoots of chestnut (Figure 26 and 27). p value = 0.0002<0.05, results are significantly different (Appendix VI, Figure 44).

Figure 26 - Evaluation of lesions in chestnut shoots inoculated with plugs of Cast13, VBC02, Cast13c, VBC02c and RB111, six days post-inoculation.
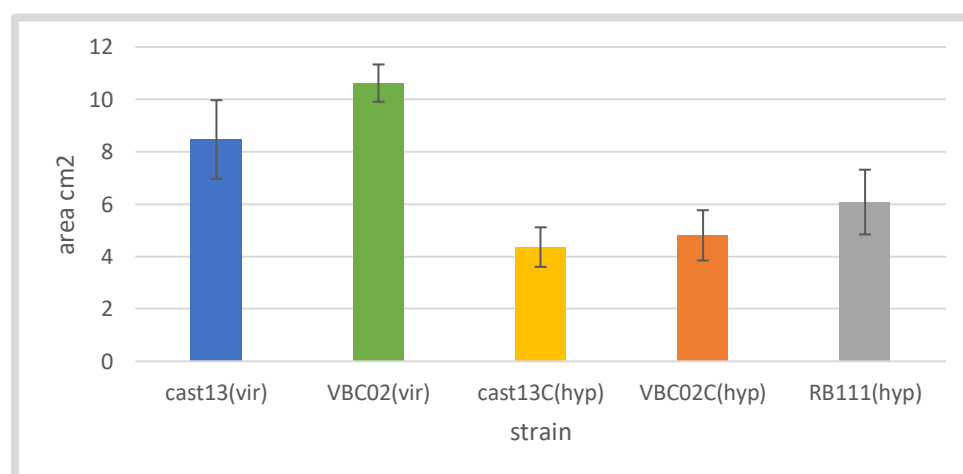
Figure 27 - Mean lesion area made by virulent and hypovirulent strains of *Cryphonectria parasitica* after 6 days of inoculation.

1.3 CHV1 identification

Two converted strains were tested for the presence of dsRNA (one hypovirulent was used as a control) using two types of primers ORF region A and ORF region B. All strains contained dsRNA using ORF A and ORF B primers (Figure 28). The 3 hypovirulent strains (original and converted) are infected by the virus.
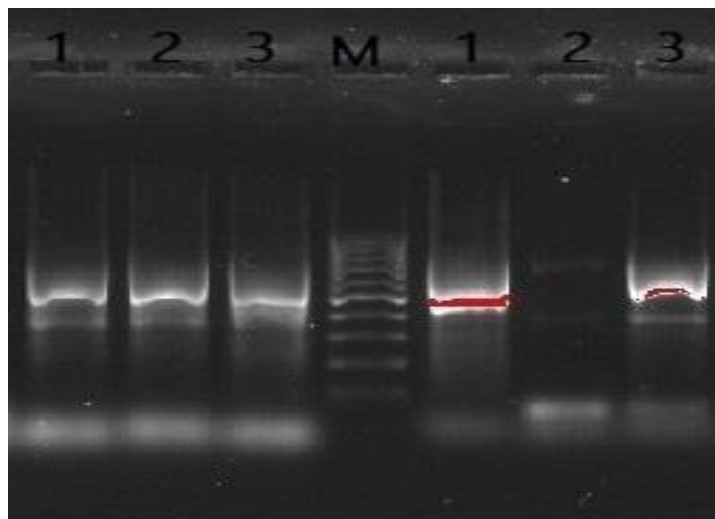
Figure 28 - CHV1 detection in hypovirulent strains of *C. parasitica* using two different primers ORFA (right) and ORFB (left). (1: Cast13c; 2: RB111; 3: VBC02; M: marker)

2.   Qualitative and quantitative evaluation of ligninolytic enzyme production

The differences in laccase, cellulase and lignin peroxidase production for nine different strains are shown in Figures 29 and 30, and compared in Table 3. The positive results with Azure B and RBBR are observed as colorless halos around microbial growth, which indicates the production of lignin-degrading enzymes, with simultaneously coloration of the mycelium by the dye, as shown in Figure 30. A positive cellulase test is indicated by the formation of a yellow halo after flooding the plate with Congo Red (Figure 29 B). A positive Bavendamm test results is a brown color around the microbial growth indicating a polyphenol oxidase activity (Figure 29 A).

The analysis of Table 3 reveals that virulent strains (Cast13 EU11, Cast26 EU11, VBC02 EU11, Cast07 EU66, Cast17 EU66, VDP11 EU66) showed more intensive color and/or bigger halos for all the indicators used than hypovirulent strains (RB111, Serra05, SR442) indicating higher production of lignin-degrading enzymes and cellulase.

2.1 Qualitative evaluation: Dyes decolorization
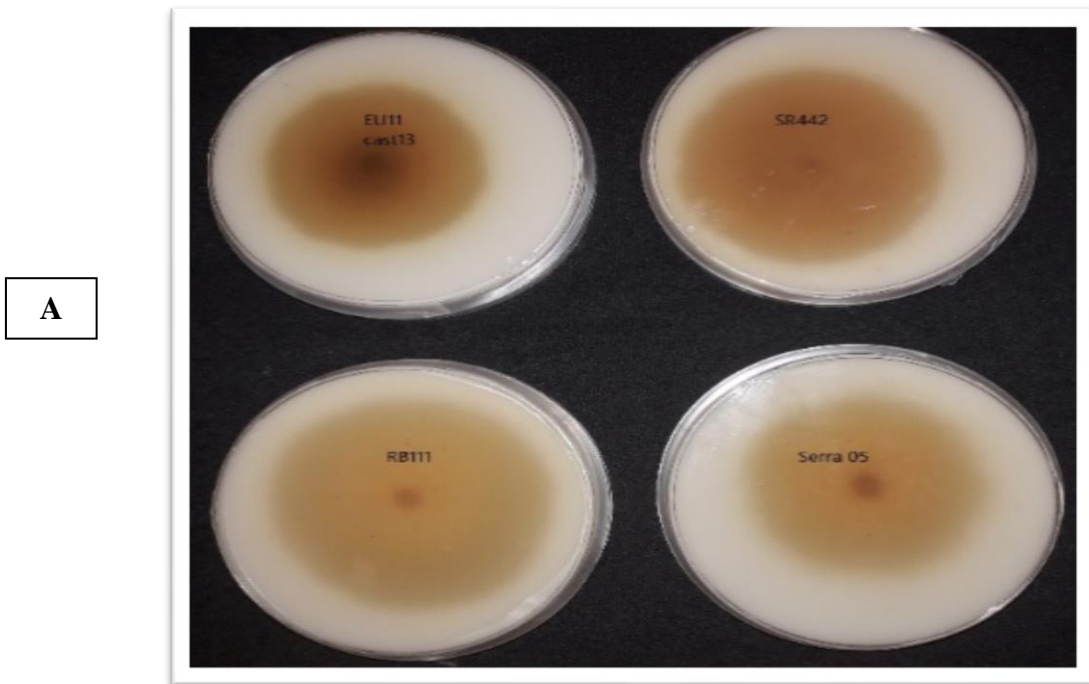
Figure 29 – A: Four of the nine isolates tested for Bavendamm test; B: Cellulase test.
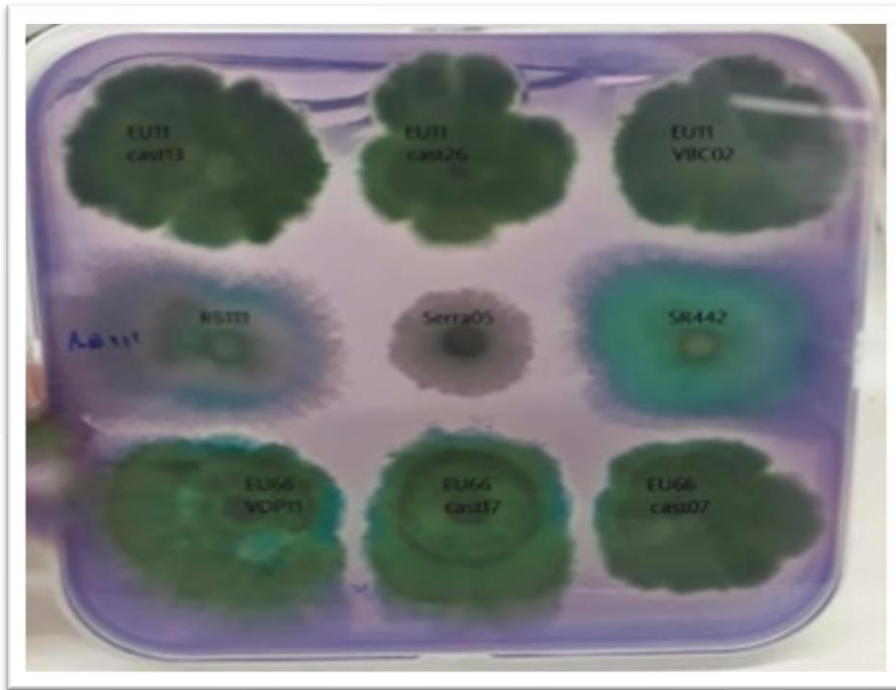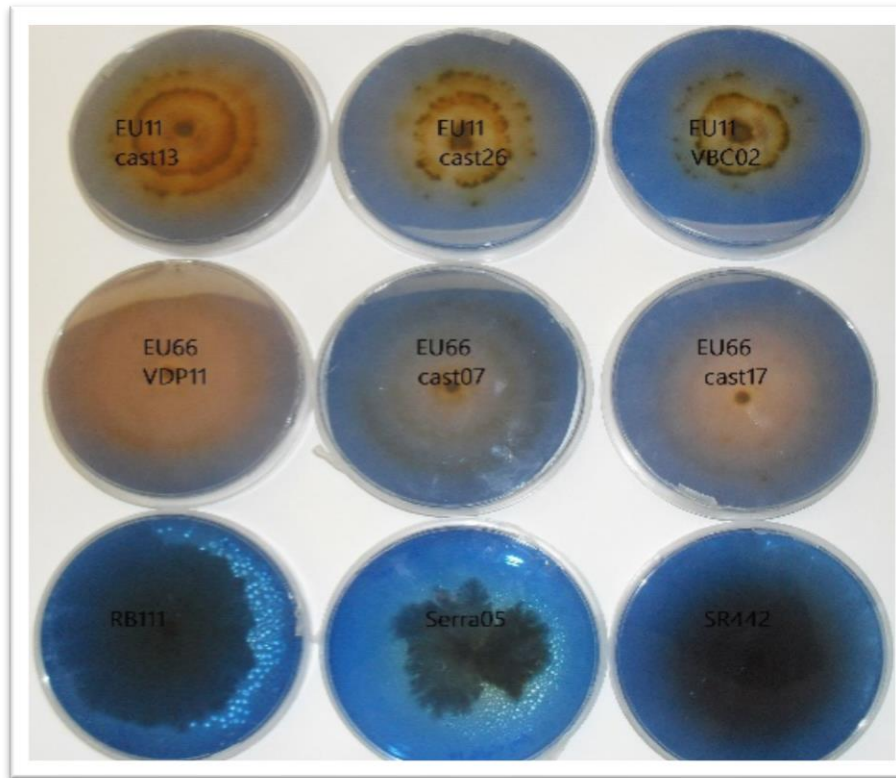
Figure 30 - A: Azure B dye; B: RBBR dye.

Table 3 - Effect on dyes decolorization during growth of different fungal strains

Strains	Bavendamm	Cellulase	Azure B	RBBR
Cast13 (EU11)	+++	2	+++	+++
Cast26 (EU11)	+++	2	+++	+++
VBC02 (EU11)	+++	2	+++	++
RB111	+	1	+	+
Serra05	+	1	+	+
SR442	++	1	+	+
Cast07 (EU66)	+++	3	+++	+++
Cast17 (EU66)	+++	3	+++	+++
VDP11 (EU66)	+++	3	+++	+++

Bavendamm test: + to +++ refer to increasing color reaction obtained in the test.
Halo diameter in cellulase test: 1→ refer small (5-14mm) ø halo, 3→big (15-25mm) ø halo.
Dye decolorization in Azure B and RBBR medium: + to +++ refer to increasing decolorization.

2.2 Quantitative evaluation

Specific laccase activity for five chosen strains are shown in Figure 32, 34, absorbance curves are presented in Figure 31 and 33, enzymes measurement and data are shown in Appendix I, Table 5, 6, 7, 8, 9 and 10.
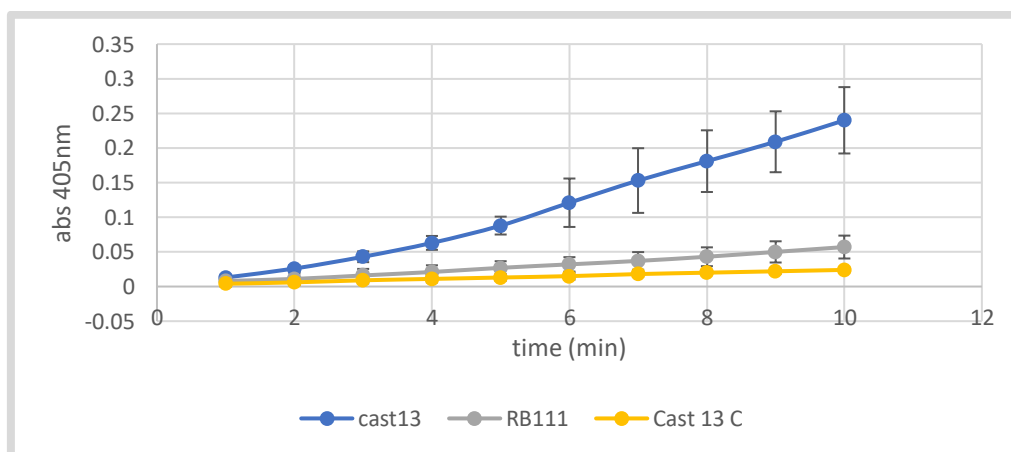
Figure 31 - Change in absorbance at 405nm of 3 strains of *Cryphonectria parasitica*.
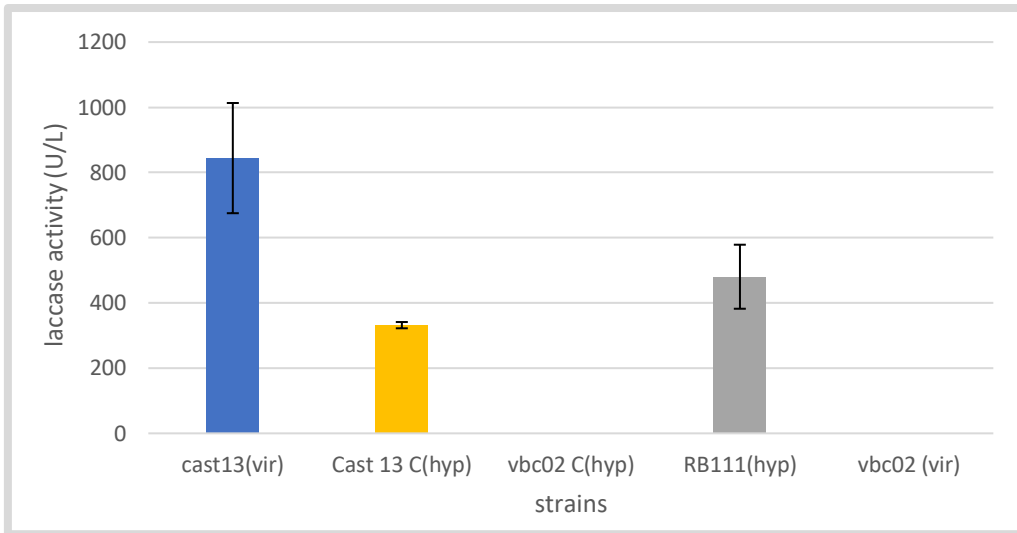
Figure 32 - Specific laccase activity for the first culture.
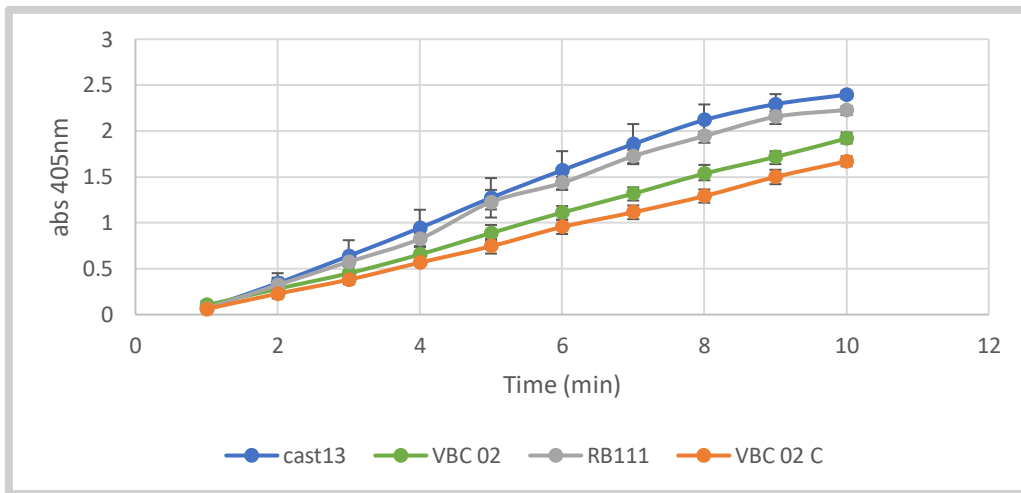
Figure 33 - Change in absorbance at 405nm of 4 strains of *Cryphonectria parasitica*
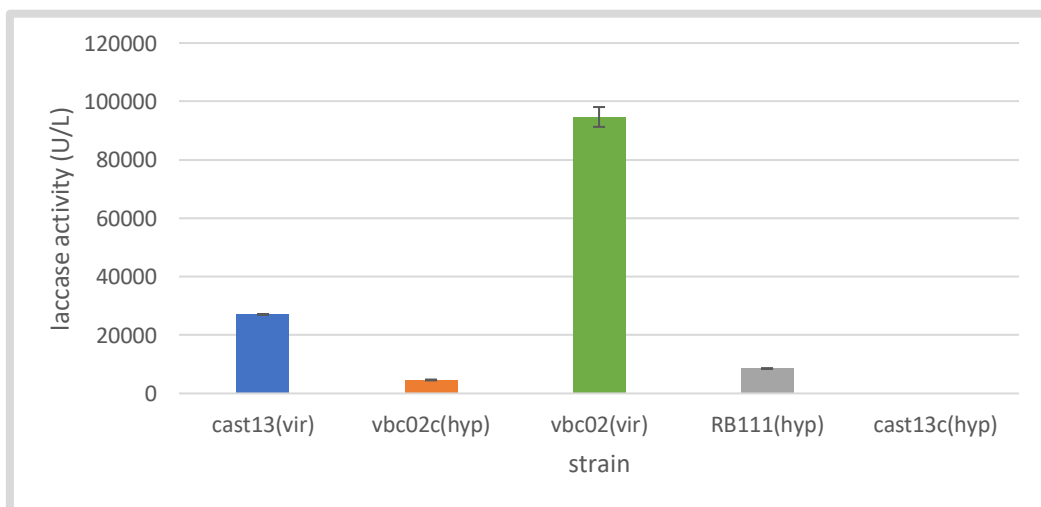
Figure 34 - Specific laccase activity of the second culture.

For the second culture, the virulent strain VBC02 had the highest specific laccase activity followed by the virulent strain Cast13, the converted strain Cast13c had the lowest specific laccase activity for the 1st culture and VBC02c for the 2nd. The difference in the enzyme specific activity was huge between the 2 cultures. Some strains didn't show any activity in one of the cultures caused by instant degradation or adsorption of the substrate ABTS. p value = 0.0036<0.05 for the first culture and 0<0.05 for the second culture, results are significantly different (Appendix VI, Figure 46 and 47).

Specific lignin peroxidase activity for five chosen strains are shown in Figure 36, absorbance curves are presented in Figure 35, The measurement data and calculation of lignin peroxidase activity is given in Appendix I, Table 11, 12, 13 and 14.
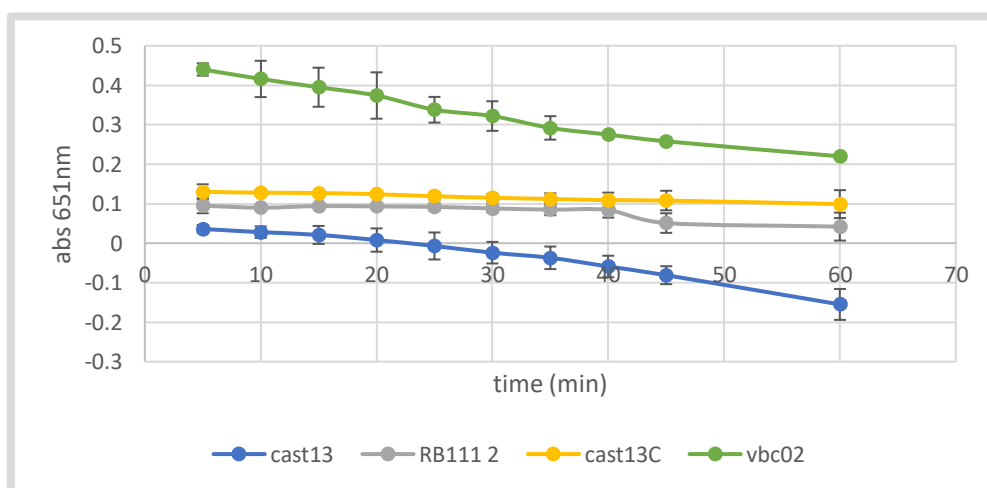
Figure 35 - Change in absorbance at 651nm of 4 strains of *Cryphonectria parasitica.*
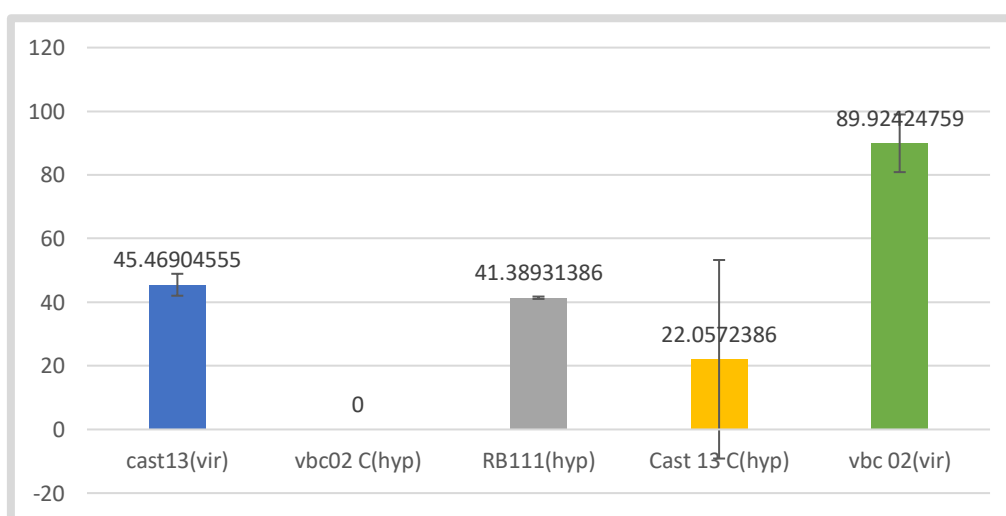
Figure 36- Specific Lignin peroxidase activity for 5 strains of *C. parasitica.*

The highest amount of lignin peroxidase was produced by the wild type strain VBC02 and the lowest by dsRNA containing strain Cast13, which also have a great margin of error caused by a very different absorbance values between the repetitions as shown in Figure 36. The converted strain VBC02c didn't produce any lignin peroxidase. In the second culture, all strains had no LiP activity. These observations were confirmed by the calculation of specific enzyme activity, expressed by μmole per milligram of protein and minute (U/mg), using total protein content of the growth medium presented in Appendix II. Manganese peroxidase presents different absorbance values in the first minute caused by the addition of the supernatant, after some minutes all curves started to tend toward zero showing no MnP activity. p value = 0.0002<0.05, results are significantly different (Appendix VI, Figure 47).

3. BIOLOG microplates: metabolic profiles characterization

All BIOLOG measurement and Data are presented in Appendix V. We have 95 carbon sources, 75 of them were used by all the strains. None of the 5 strains was able to consume all types of substrates. All strains were unable to utilize just one carbon source: 2-amino ethanol, the virulent strain VBC02 consumed less carbon sources than all other strains (85 carbon sources), the hypovirulent strain RB111 consumed the most carbon sources (93 carbon sources). Cast13c had the highest average well color development (AWCD) after 7 days of inoculation (Figure 37).
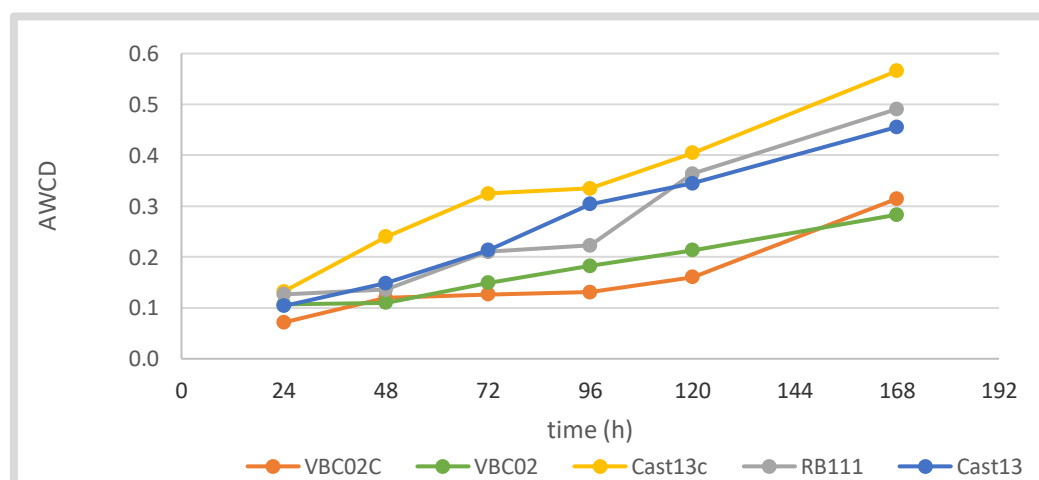
Figure 37 - Average well color development for the five strains after seven days of inoculation.
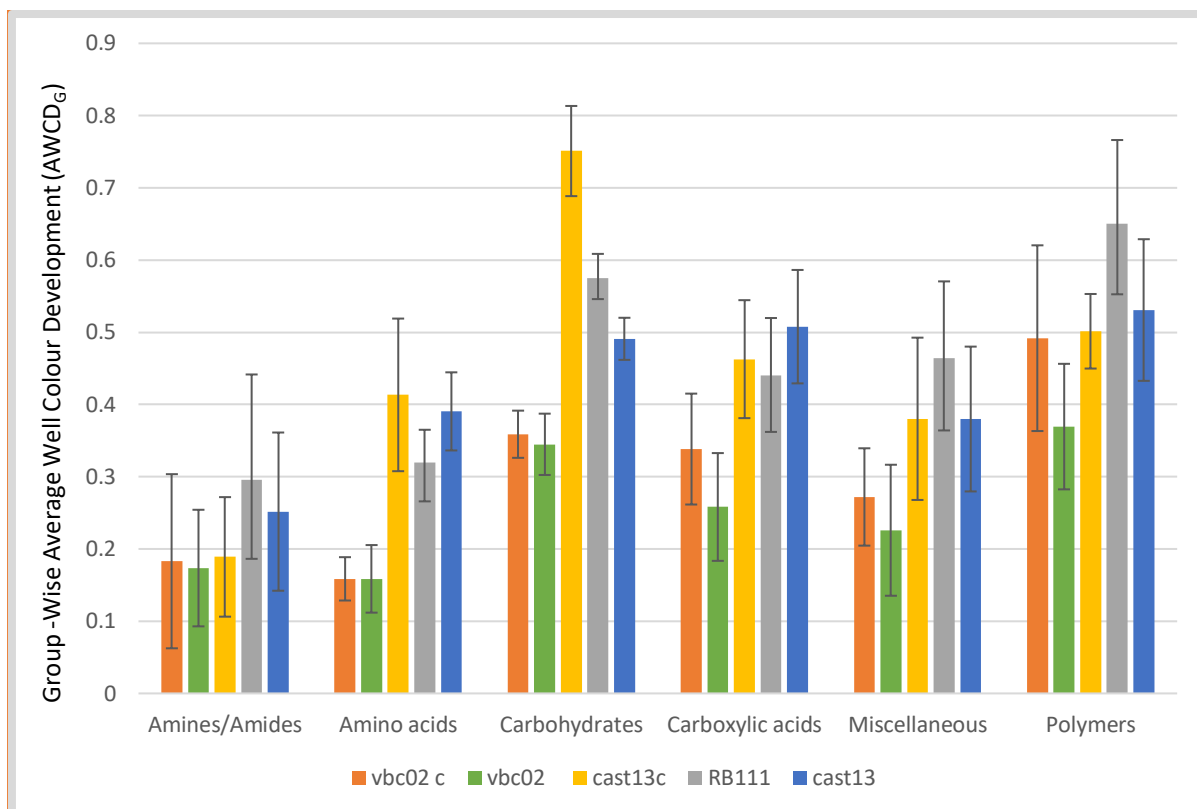
Figure 38 - Diagram of carbon sources utilization, by chemical groups, for 5 strains of
Cryphonectria parasitica after seven days of inoculation.

Figure 38 shows the differences in chemicals groups consumption by five strains of
Cryphonectria parasitica 2 virulent (Cast13, VBC02) their converted ones (Cast13c,
VBC02c) and RB111. Cast13 converted is the strain that utilize the most amino acids and
carbohydrates. Hypovirulent strain RB111 has dominance in the consumption of
amines/amides, miscellaneous and polymers composts. Cast 13 develops the most color
intensity for carboxylic acids, comparing to the other strains. VBC02 shows the less
consumption of carbon sources.

The heat map representing carbon source utilisation by *Cryphonectria parasitica* strains
are presented in Figure 39:
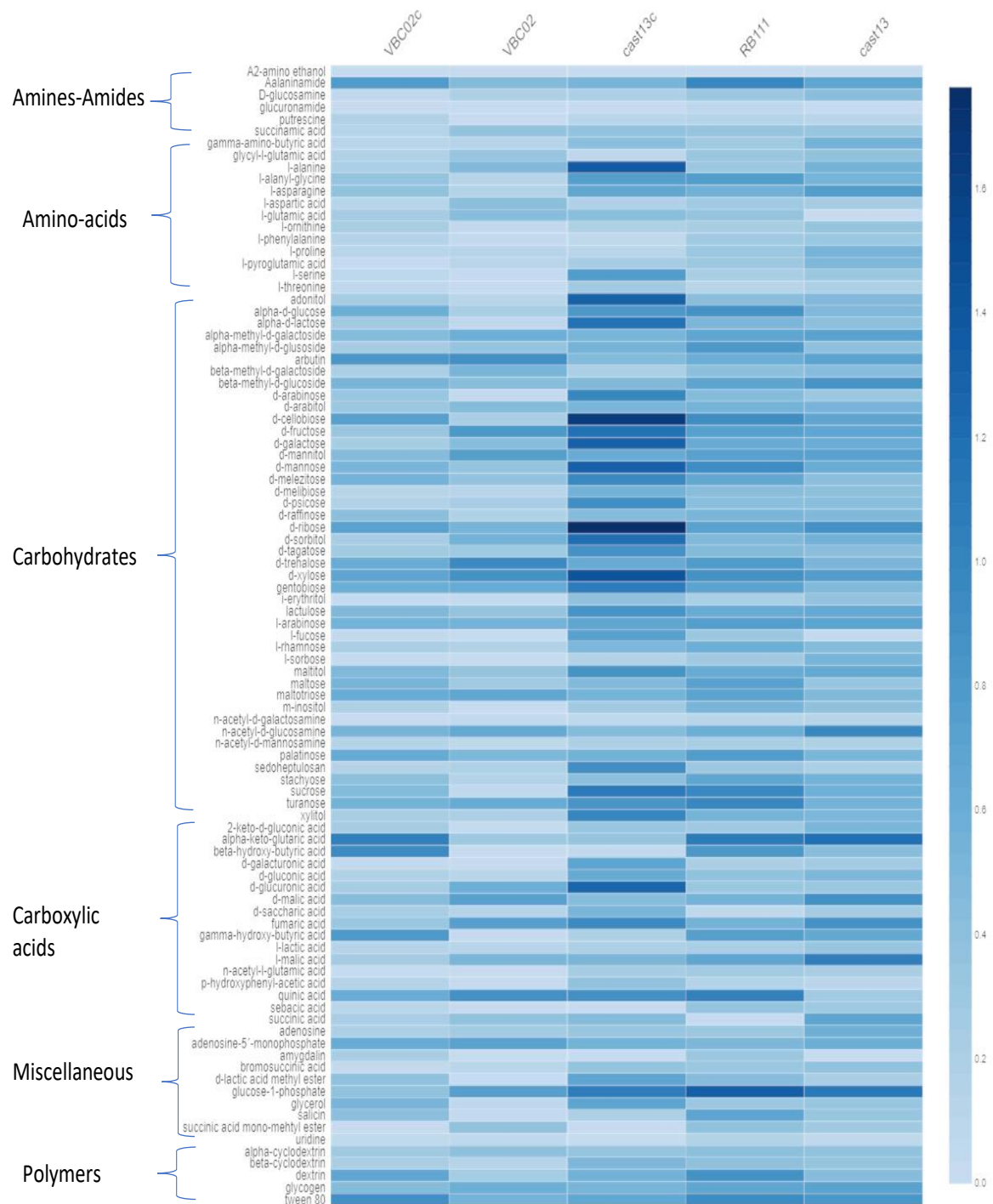
Figure 39 - Heat map of carbon source utilisation by *Cryphonectria parasitica* strains assessed through Well Color Development (WCD) at seven days, corrected to control, of each of 95 carbon sources/chemical group, using Biolog FF MicroPlates.

Table 4 - Principal component: Eigenvalue and variance

PC	Eigenvalue	% variance
1	3.28969	57.453
2	1.28441	22.432
3	0.738476	12.897
4	0.413284	7.2179
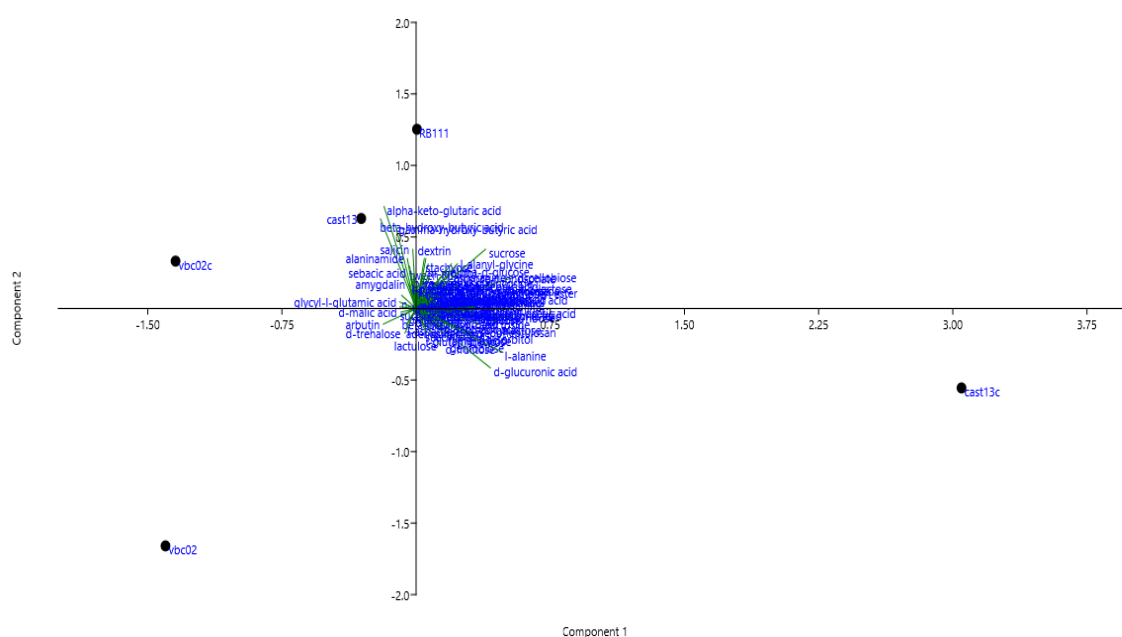
Figure 40 - Principal Component Analysis of carbon utilisation obtained through Biolog FF Microplates for *Cryphonectria parasitica* isolates.

The PCA analysis (Figure 40) shows that the strains studied have large differences in their metabolic profiles, specially Cast13c and VBC02 which are located in different quadrants. RB111, Cast13 and VBC 02 are relatively related.

V. Discussion

This project aims to compare virulent strains of *Cryphonectria parasitica* with virus infected strains, the hypovirulent strains, utilized as biological control agents.

Nine different fungal strains were screened on PDA media containing colored indicator compounds that enabled the visual detection of ligninolytic enzymes production. Several different compounds have been used as indicators for ligninolytic enzymes production. These compounds and indicators were more consumed by virulent strains of *C. parasitica* than by hypovirulent ones, enhancing the difference in phenol oxidase activity after the transfer of the dsRNA into virulent strains, as it has been reported for the Bavendamm test (Rigling *et al.*, 1989). The comparable growth rate of virulent and hypovirulent strains in the Bavendamm test or in the Azure B test prove that dsRNA affects phenol oxidase activities but not general viability of the strains.

Five strains (two virulent, three hypovirulent - two converted and one original) were selected for further studies for the reason that these strains showed great differences in the qualitative evaluation and they belong to the same VCG group (EU11) which resulted in a successful conversion. These strains were inoculated in different materials, namely apples and chestnut branches, to characterize their degree of virulence. Results obtained from the chestnut branches inoculation were related with the ones obtained previously with the indicators of ligninolytic enzymes production. Chestnut shoots are composed of lignin, hemicellulose and cellulose therefore the lesions made by virulent strains, which have higher laccase activity, were more important than the damage made by strains that contains dsRNA, which suffer from decrease in laccase activity, consequently a laccase-null mutant caused a smaller lesion area on chestnut bark than did the wild type (Chung *et al.*, 2008). The reduction in the lesion area made by hypovirulent strains was also tested and proved in other studies, for *C. parasitica* (Chung *et al.*, 2008) and other phytopathogenic fungus (Zhai *et al.*, 2016). Besides that, the biggest rot lesion was made by a virulent strain VBC 02, and the smallest by a hypovirulent VBC 02c, Different results were attained in the case of apple fruits inoculation by a converted strain Cast13c, which made bigger infection area than its virulent version Cast13. This observation can be related to the one reported with the BIOLOG microplate that shows a high carbohydrates degradation by some hypovirulent strain, especially Cast13c. Carbohydrates represents the principal component of an apple. Some of the hypovirulent strains tested showed great

carbohydrates consumption but small rot lesion in the apple. The reason for that can be due to the types of carbohydrates presents in the apple and the different affinity for these substrates by *C. parasitica* strains.

Two similar cultures medium were made to measure the activity of 3 ligninolytic enzymes secreted by the 5 strains chosen previously. The amount of Laccase and LiP produced by wild type strains was high compared to dsRNA containing strains, for laccase (844 U/mg in Cast13, 331 U/mg in Cast13c for 1st culture), (94680 U/mg in VBC02, 4608 U/mg in VBC02c in the 2nd culture), for LiP (45 U/mg in Cast13, 22U/mg in Cast13c) and for MnP no activity was detected in the 2nd culture media suggesting that *C. parasitica* belongs to the type of fungus who are able to degrade lignin by producing laccase and lignin peroxidase (Dashtban *et al*., 2010). Laccase play a role in the infection process and are involved in the degradation of lignin, pathogenesis, formation of fruiting body and pigmentation (Rigling and Prospero, 2017). The locus controlling the functions mentioned previously could be one that controls phenol oxidase activity of the laccase and lignin peroxidase type which is affected by dsRNA in white strains. The hypothesis saying that laccase activity is reduced by the presence of dsRNA was proved by many studies before (Rigling *et al.*, 1989; Rigling and Alfen, 1993; Chung *et al*., 2008), but Lignin peroxidase and manganese peroxidase activity for *C. parasitica* have never been studied before. We can notice the huge activity differences given by the 2 culture, which can be a consequence of the dissimilarity between the chestnut branches, used as inducers. Actually, some studies have related radial growth rates to blight susceptibility (Reynolds *et al*., 2011), or the presence of some inhibitors in the growth medium (Eggert *et al*., 1996). VBC02, VBC02c in the 1st culture, Cast13c in the 2nd culture, showed both no activity and instant disappearance of the substrate ABTS after adding the supernatant, some ABTS-degrading substances may be present in this liquid.

At the metabolic level, their metabolic profiles were evaluated using Biolog FF MicroPlates, with concurrent reads of fungal utilization of 95 different carbon sources. Hypovirulent strains showed great consumption of some chemical groups and very different metabolic profile comparing to their virulent version. This hypovirulent strains are infected by the mycovirus CHV1, which is known to reduce the pathogenicity of the fungal but without completely dysfunction the mycelium. In contrary, the virus somehow looks like to keep the mycelium in a juvenile state with the induction of some metabolic pathways, while the debilitation is affecting pathways related to the virulence of the fungi. These observations are supported by our results: amines/amides, miscellaneous and

polymers, amino acids and carbohydrates are more consumed by hypovirulent strains than by virulent strains. Other study also proved that the consumption of some amino acids, carbohydrates, lipids and nucleotides are increased in a virus infected *C. parasitica* comparing to wild type strain (Dawe *et al.*, 2009). The infection activates some metabolic pathways included in the fungal defense mechanism against the mycovirus. Some of these pathways require amino acids to produce antiviral toxins, they consume also different carbohydrates, which gives the mycelium the ability to take other pathways to produce energy or other compounds, and that explain the result from PCA analysis that shows the big difference in the metabolic profiles between a virulent and its white strain.

C. parasitica isolates variability was assessed using Biolog FF MicroPlates for the first time. The use of this metabolic approach may facilitate future dsRNA detection, as the use of different carbon sources by one converted isolate, comparing to its virulent type, may confirm the transfer of the dsRNA.

VI. Conclusion

Two wild strains of *C. parasitica* were converted using an hypovirulent strain, then two virulent and three hypovirulent strains were chosen to test their pathogenicity and ligninolytic enzymes production. Results showed that damage on chestnut branches made by dsRNA containing strains is smaller than the one done by virulent strains, in addition laccase and lignin peroxidase activities are reduced in hypovirulent strains. However, metabolic profiles evaluation assessed by BIOLOG microplates revealed that most of carbon sources are more consumed by hypovirulent strains. The aforementioned achievements lead to the conclusion that mycovirus don't cause a general debilitation of the fungus but they partially modify the genes related to the pathogenicity.

Our metabolic analysis, the first time used on *Cryphonectria parasitica,* has revealed the enormous changes that happens in response to the hypovirus, it may also facilitate future isolate selection, as the use of specific carbon sources provides complete information on the isolates, which enable the insertion of such information in a scientific database. These studies may lead to new perspectives for understanding the biological process used by the hypovirus.

VII. References

Anagnostakis S. L. 1977. Vegetative Incompatibility in Endothia parasitica. Experimental Mycology 1(1):306–16.

Anagnostakis S. L. 1992. Measuring Resistance of Chestnut Trees to Chestnut Blight. Canadian Journal of Forest Research 22(4):568–71.

Arora D. S. and Gill P. K. 2001. Comparison of Two Assay Procedures for Lignin Peroxidase. Enzyme and Microbiol Technology 28:602–5.

Arora D. S. and Sharma R. K. 2010. Ligninolytic Fungal Laccases and Their Biotechnological Applications. Applied Biochemistry and Biotechnology 160(6):1760–88.

Badal C. S. 2000. Alpha L -Arabinofuranosidases : Biochemistry , Molecular Biology and Application in Biotechnology. Biotechnology Advances 18:403–23.

Biella S., Smith M. L., Aist J. R., Cortesi P. and Milgroom M. G. 2002. Programmed Cell Death Correlates with Virus Transmission in a Filamentous Fungus. Proceedings of the Royal Society 269(1506):2269–76.

Bragança H., Simões S., Santos N., Marcelino J., Tenreiro R. and Rigling D. 2005. Chestnut Blight in Portugal - Monitoring and vc Types of *Cryphonectria parasitica*. Acta Hortic 693:627–34.

Chen C., Sun Q., Narayanan. B., Nuss D. L. and Herzberg O. 2010. Structure of Oxalacetate Acetylhydrolase, a Virulence Factor of the Chestnut Blight Fungus. Journal of Biological Chemistry 285(34):26685–96.

Chung H-J., Kwon B-R., Kim J-M., Park S-M., Park J-K., Cha B-J., Yang M-S. and Kim D-H. 2008. A Tannic Acid-Inducible and Hypoviral-Regulated Laccase3 Contributes to the Virulence of the Chestnut Blight Fungus *Cryphonectria parasitica*. Molecular Plant-Microbe Interactions *: MPMI* 21(12):1582–90.

Cortesi P. and Milgroom M. G. 1998. Genetics of Vegetative Incompatibility in *Cryphonectria parasitica* Genetics of Vegetative Incompatibility. Applied and Environmental Microbiology 64(8):2988–94.

Dashtban M., Schraft H., Syed T. A. and Qin W. 2010. "Fungal Biodegradation and

Enzymatic Modification of Lignin. International Journal of Biochemistry and Molecular Biology 1(1):36–50.

Dawe, A. L., Van Voorhies W. A., Lau T. A., Ulanov A. V. and Li Z. 2009. Major Impacts on the Primary Metabolism of the Plant Pathogen *Cryphonectria parasitica* by the Virulence-Attenuating Virus CHV1-EP713. Microbiology Society 155:3913–21.

Deng F., Allen T. D. and Nuss D. L. 2007. Ste12 Transcription Factor Homologue CpST12 Is Down-Regulated by Hypovirus Infection and Required for Virulence and Female Fertility of the Chestnut Blight Fungus *Cryphonectria parasitica*. American Society for Microbiology 6(2):235–44.

Dutech, C., Fabreguettes O., Capdevielle X. and Robin C. 2009. Multiple Introductions of Divergent Genetic Lineages in an Invasive Fungal Pathogen , *Cryphonectria parasitica*, in France. Heredity 105(2):220–28.

Eggert C., Temp U. and Eriksson K-e. L. 1996. The Ligninolytic System of the White Rot Fungus *Pycnoporus cinnabarinus* : Purification and Characterization of the Laccase. American Society for Microbiology 62(4):1151–58.

Elliott K. J. and Swank W. T. 2008. Long-Term Changes in Forest Composition and Diversity Following Early Logging (1919-1923) and the Decline of American Chestnut (*Castanea dentata*). Plant Ecology 197:155–72.

Gao K., Xiong Q., Xu J., Wang K. and Wang K. 2013. CpBir1 Is Required for Conidiation , Virulence and Anti-Apoptotic Effects and Influences Hypovirus Transmission in *Cryphonectria parasitica*. Fungal Genetics and Biology 51:60–71.

Gao S., Choi G. H., Shain L. and Nuss D. L. 1996. Cloning and Targeted Disruption of Enpg-1, Encoding the Major In Vitro Extracellular Endopolygalacturonase of the Chestnut Blight Fungus, *Cryphonectria parasitica*. American Society for Microbiology 62(6):1984–90.

Griffin G. J. 1986. Chestnut Blight and Its Control. Horticultural Reviews 8:291–336.

Galhaup C. and Haltrich D. 2001. Enhanced Formation of Laccase Activity by the White-Rot Fungus Trametes Pubescens in the Presence of Copper. Applied Microbiology and Biotechnology 56:225–32.

Hillman B. I. and Suzuki N. 2004. Viruses of the Chestnut Blight Fungus, *Cryphonectria*

parasitica. Advances in Virus Research 63:423–72.

Kaczmarek B. and Kwiatos N. 2017. Laccases – Enzymes with an Unlimited Potential. Biotechnology and Food Science 81(1):41–70.

Kersten P. J., Kalyanaraman B., Hammel K. E., Reinhammar B. and Kirk T. K. 1990. Comparison of Lignin Peroxidase , Horseradish Peroxidase and Laccase in The Oxidation of Methoxybenzenes. The Biochemical Journal 268:475–80.

Kirkland B. H., Eisa A. and Keyhani N. O. 2005. Oxalic Acid as a Fungal Acaricidal Virulence Factor. Journal of Medical Entomology 42(3):346–51.

Marra R. E., Cortesi P., Bissegger M. and Milgroom M. G. 2004. Mixed Mating in Natural Populations of the Chestnut Blight Fungus, *Cryphonectria parasitica*." Heredity 93:189–95.

Milgroom M. G. and Cortesi P. 2004. Biological Control of Chestnut Blight with Hypovirulence : A Critical Analysis. Annual Reviews 42(102):311–38.

Monteiro M. L. 2000. Trás-os-Montes um lugar de Castanheiros. In: Pereira R (ed) Florestas de Portugal. Direcção Geral das Florestas, Lisboa

Myburg H., Gryzenhout M., Wingfield B. D. and Milgroom M. G. 2004. DNA Sequence Data and Morphology Define *Cryphonectria* Species in Europe , China and Japan. Canadian Journal of Botany 82:1730–43.

Nakagawa Y. and Shimazu K. 1999. *Aspergillus niger pneumonia* with Fatal Pulmonary Oxalosis. Journal of Infection and Chemotherapy 5(2):97–100.

Onofre N., Tenreiro R., and Rigling D. 2007. *Cryphonectria parasitica* in Portugal : Diversity of Vegetative Compatibility Types , Mating Types , and Occurrence of Hypovirulence. Forest Pathology 37(6):391–402.

Park S-M., Choi E-S., Kim M-J., Cha B-J., Yang M-S. and Kim D-H. 2004. Characterization of HOG1 Homologue , CpMK1 , from *Cryphonectria parasitica* and Evidence for Hypovirus- Mediated Perturbation of Its Phosphorylation in Response to Hypertonic Stress. Molecular Microbiology 51(5):1267–77.

Prospero S. and Rigling D. 2013. Chestnut Blight. In: Infectious Forest Diseases. Pp. 318–38 in Infectious Forest Disease*s*, edited by G. Gonthier, P. and Nicolotti. CAB international.

Prospero S., Conedera M., Heiniger U. and Rigling D. 2006. Saprophytic Activity and Sporulation of *Cryphonectria parasitica* on Dead Chestnut Wood in Forests with Naturally Established Hypovirulence. The American Phytopathological Society 96(12):1337–44.

Reynolds D. L., Burke K. L. 2011. The Effect of Growth Rate, Age, and Chestnut Blight on American Chestnut Mortality. Castanea 76(2):129–39.

Rice A. V. and Currah R. S. 2005. Profiles from Biolog FF Plates and Morphological Characteristics Support the Recognition of *Oidiodendron fimicola* Sp . Nov. Studies in Mycology 53:75–82.

Rigling D., Heiniger U., Hohl H. R. 1989. Reduction of Laccase Activity in DsRNA-Containing Hypovirulent Strains of *Cryphonectria* (*Endothia*) *parasitica*. Phytopathology 79:219–23.

Rigling, D. and Prospero S. 2017. *Cryphonectria parasitica*, the Causal Agent of Chestnut Blight: Invasion History, Population Biology and Disease Control. Molecular Plant Pathology 9(20 18):7–20.

Rigling, D. and Alfen N. K. 1993. Extra- and Intracellular Laccases of the Chestnut Blight Fungus, *Cryphonectria parasitica*. Applied and Enviromental Microbiology 59(11):3634–39.

Rivera-Hoyos C. M., Morales-Álvarez E. D., Poutou-Piñales R. A., Pedroza-Rodríguez A. M., RodrÍguez-Vázquez R. and Delgado-Boada J. M. 2013. Fungal Laccases. Fungal Biology Reviews 27(3–4):67–82.

Robin C. and Heiniger U. 2001. Chestnut Blight in Europe : Diversity of *Cryphonectria parasitica* , Hypovirulence and Biocontrol. Forest Snow and Landscape Research 76(3):361–67.

Rouane M.K, Griffin G.J and Elkins J. 1986. Chestnut Blight, Other *Endothia* Diseases, and the Genus *Endothia.* St. Paul, Minnesota.

Ruiz-Dueñas F. J., Morales M., Garcia E., Miki Y., Martinez M. J. and Martinez A. T.

2009. Substrate Oxidation Sites in Versatile Peroxidase and Other Basidiomycete Peroxidases. Journal of Experimental Botany 60(2):441–52.

Salamon J. A., Acuña R. and Dawe A. L. 2010. Phosphorylation of Phosducin-like Protein BDM-1 by Protein Kinase 2 (CK2) Is Required for Virulence and G b Subunit Stability in the Fungal Plant Pathogen *Cryphonectria parasitica*. Molecular Microbiology 76(4):848–60.

Santos C. 2017. Genomic approaches to understand the genetic response to *Phytophthora cinnamomi* Rands in Castanea spp. Instituto de Tecnologia Química e Biológica António Xavier

Smith A. R. 2013. Biological Control of *Cryphonectria parasitica* with Streptomyces and an Analysis of Vegetative Compatibility Diversity of *Cryphonectria parasictica* in Wisconsin, USA. University of Wisconsin-La Crosse.

Speranza M., Ruiz-Dueñas F. J., Ferreira P., Camarero S., Guillén F., Gutiérrez A. and Río J. C. 2005. Biodegradation of Lignocellulosics : Microbial, Chemical, and Enzymatic Aspects of the Fungal Attack of Lignin. International Microbiology 8(3):195–204.

Srebotnik E., Messner K. and Foisner R. 1988. Penetrability of White Rot-Degraded Pine Wood by the Lignin Peroxidase of *Phanerochaete chrysosporium*. Applied and Environmental Microbiology 54(11):2608–14.

Swe K. T. 2011. Screening of Potential Lignin-Degrading Microorganisms and Evaluating Their Optimal Enzyme Producing Culture Conditions. Chalmers University of Technology.

Tanaka H., Itakura S. and Enoki A. 1999. Hydroxyl Radical Generation by an Extracellular Low-Molecular-Weight Substance and Phenol Oxidase Activity during Wood Degradation by the White-Rot Basidiomycete *Trametes versicolor*. Journal of Biotechnology 75(1):57–70.

Tarcali G. 2007. Examination of *Cryphonectria parasitica* (MURRILL) M.E. Barr in the Carpathian-Basin. Debrecen University.

Thurston C. F. 1994. The Structure and Function of Fungal Laccases. Microbiology 140:19–26.

Trapiello E., González-varela G. and González A. J. 2015. Chestnut Blight Control by Agrochemicals in *Castanea Sativa* under Managed Conditions. Journal of Plant Diseases and Protection 122(3):4–5.

Turina M. and Rostagno L. 2007. Virus-Induced Hypovirulence in *Cryphonectria parasitica* : Still Unresolved Conundrum." Journal of Plant Pathology 89(2):165–78.

Wang L., Wenchao Y., Jiachuan C., Feng H. and Peiji G. 2008. Function of the Iron-Binding Chelator Produced by Coriolus Versicolor in Lignin Biodegradation. 51(3).

Wei H., Xu Q., Taylor Ii L. E., Baker J. O., Tucker M. P., and Ding S-Y. 2009. Natural Paradigms of Plant Cell Wall Degradation. Current Opininon in Biotechnology. 20(3):330–80.

Wesenberg, D., Kyriakides I. and Agathos S. N. 2003. White-Rot Fungi and Their Enzymes for the Treatment of Industrial Dye Effluents. Biotechnology Advances 22(1–2):161–87.

Wong D. W. 2009. Structure and Action Mechanism of Ligninolytic Enzymes. Applied Biochemistry and Biotechnology 157(2):174–209.

Zhai L., Xiang J., Zhang M., Fu M., Yang Z. and Hong N. 2016. Characterization of a Novel Double-Stranded RNA Mycovirus Conferring Hypovirulence from the Phytopathogenic Fungus *Botryosphaeria dothidea*. Virology 493:75–85.

VIII. Appendix

Appendix I: Calculation for laccase, lignin peroxidase and manganese peroxidase activities

Table 5 - Absorbance at 405 nm for laccase activity for the first culture

strain	N° / tmin	1	2	3	4	5	6	7	8	9	10
Cast13	1	0.013	0.024	0.038	0.055	0.074	0.095	0.118	0.145	0.171	0.198
	2	0.017	0.032	0.052	0.074	0.099	0.161	0.206	0.231	0.257	0.292
	3	0.01	0.023	0.039	0.059	0.092	0.108	0.135	0.168	0.198	0.229
	average	0.013	0.026	0.043	0.063	0.088	0.121	0.153	0.181	0.209	0.240
RB111	1	0.007	0.009	0.013	0.017	0.021	0.026	0.03	0.035	0.041	0.046
	2	0.017	0.019	0.027	0.032	0.038	0.044	0.052	0.059	0.068	0.076
	3	0.001	0.004	0.009	0.014	0.022	0.026	0.03	0.036	0.042	0.049
	average	0.008	0.011	0.016	0.021	0.027	0.032	0.037	0.043	0.05	0.057
Cast13 (C)	1	0.001	0.002	0.004	0.006	0.008	0.01	0.014	0.017	0.018	0.02
	2	0.007	0.01	0.013	0.016	0.017	0.02	0.021	0.023	0.025	0.027

| | **3** | 0.004 | 0.007 | 0.009 | 0.012 | 0.014 | 0.016 | 0.018 | 0.02 | 0.022 | 0.024 |
| | **average** | 0.004 | 0.006 | 0.009 | 0.011 | 0.013 | 0.015 | 0.018 | 0.02 | 0.022 | 0.024 |

Table 6 - Absorbance at 405 nm for laccase activity for the second culture

strain	N°⟋tmin	1	2	3	4	5	6	7	8	9	10
Cast13	**1**	0.074	0.459	0.825	1.154	1.494	1.778	2.035	2.22	2.391	2.423
	2	0.075	0.243	0.489	0.76	1.065	1.362	1.613	1.923	2.174	2.345
	3	0.069	0.324	0.602	0.919	1.257	1.575	1.922	2.215	2.31	2.417
	average	0.073	0.342	0.639	0.944	1.272	1.572	1.857	2.119	2.292	2.395
VBC02	**1**	0.127	0.386	0.54	0.739	0.976	1.192	1.396	1.646	1.789	1.99
	2	0.132	0.28	0.439	0.649	0.887	1.062	1.268	1.479	1.683	1.867
	3	0.047	0.176	0.371	0.578	0.8	1.08	1.288	1.481	1.679	1.897
	average	0.102	0.281	0.45	0.655	0.888	1.111	1.317	1.535	1.717	1.918
RB111	**1**	0.08	0.397	0.646	0.854	1.351	1.445	1.768	1.962	2.21	2.275

	2	0.054	0.239	0.499	0.752	1.086	1.366	1.643	1.887	2.09	2.197
	3	0.06	0.329	0.58	0.87	1.239	1.494	1.765	1.984	2.161	2.214
	average	0.0647	0.322	0.575	0.825	1.225	1.435	1.725	1.944	2.154	2.229
VBC02 (C)	**1**	0.061	0.237	0.402	0.562	0.78	1.017	1.151	1.301	1.551	1.675
	2	0.081	0.273	0.414	0.597	0.8	0.975	1.163	1.357	1.537	1.722
	3	0.037	0.172	0.323	0.538	0.653	0.869	1.028	1.214	1.409	1.613
	average	0.06	0.227	0.380	0.566	0.744	0.954	1.114	1.291	1.499	1.67

Table 7 - Calculation of laccase activity first culture

strains	ε (M cm^{-1})	Slope (min^{-1})	Sample volume (L)	Laccase activity	
				µM per min	µM/L.min
Cast13	36780	0.025	0.25. 10^{-3}	1.03	4114.55
RB111	36780	0.005	0.25. 10^{-3}	0.22	888.16
Cast13c	36780	0.002	0.25. 10^{-3}	0.09	362.51

Table 8 - Calculation of laccase activity second culture

strains	ε (M cm^{-1})	Slope (min^{-1})	Sample volume (L)	Laccase activity	
				µM per min	µM/L.min
Cast13	36780	0.24	0.25. 10^{-3}	9.66	38640.56
VBC 02	36780	0.19	0.25. 10^{-3}	7.95	31827.07
RB111	36780	0.21	0.25. 10^{-3}	8.94	35796.63
VBC02 C	36780	0.17	0.25. 10^{-3}	6.97	27884.72

Calculation for laccase activity:

According to Lambert-Beer law:

$A = \varepsilon c l$

Where A = Absorbance

ε = Molar absorption coefficient (M-1 cm-1)

c = Concentration (M), l = path length (cm)

Given the change in absorbance per time

$\Delta c/\Delta t = \Delta A/ \varepsilon l \Delta t$, Thus, $c = \Delta A/\varepsilon l \Delta t$

Where c = Enzyme activity (M/L.min)

ΔA = Increase in absorbance at 405 nm

ε = Molar absorption coefficient =

l = path length = 1.5cm

Δ t = Reaction time in minute

Δ A/ Δ t = slope from graph

Thus,

c (μM/L.min) = (10^6 x slope)/ ε*1.5

Table 9 - Specific laccase activity first culture

strain	Laccase activity (U/L)	Total protein (mg/L)	Specific laccase activity (U/mg)
Cast13	4114.55	4.87	844.19
Cast13 c	362.51	1.09	331.84
RB111	888.16	1.84	480.41

Table 10 - Specific laccase activity second culture:

strain	Laccase activity (U/L)	Total protein (mg/L)	Specific laccase activity (U/mg)
Cast13	38640.56	1.43	27048.39
VBC02	31827.08	0.34	94685.56
RB111	35796.62	4.20	8519.60
VBC02 c	27884.72	6.05	4608.72

Specific laccase activity (U/mg) = Laccase activity (U/L)/ Total protein (mg/L)

Table 11 - Absorbance at 651 nm for lignin peroxidase activity (first culture)

strain	N° ╱ tmin	5	10	15	20	25	30	35	40	45	60
Cast13	1	0.036	0.028	0.021	0.008	-0.007	-0.024	-0.037	-0.059	-0.081	-0.155
	2	0.052	0.056	0.057	0.05	0.039	0.014	0.001	-0.025	-0.049	-0.08
	3	0.055	0.035	0.015	-0.007	-0.028	-0.039	-0.055	-0.079	-0.093	-0.137
RB111	1	0.109	0.116	0.116	0.11	0.107	0.1	0.092	0.083	0.076	0.059
	2	0.077	0.09	0.094	0.093	0.092	0.088	0.085	0.084	0.051	0.042
	3	0.165	0.178	0.177	0.17	0.168	0.164	0.16	0.152	0.14	0.12

Cast13 (C)	1	0.112	0.128	0.127	0.124	0.119	0.115	0.112	0.109	0.108	0.099
	2	-0.145	-0.14	-0.187	-0.215	-0.218	-0.238	-0.263	-0.278	-0.323	-0.382
	3	0.165	0.178	0.177	0.17	0.168	0.164	0.16	0.152	0.14	0.12
Vbc02	1	-0.102	-0.13	-0.175	-0.176	-0.207	-0.224	-0.242	-0.26	-0.274	-0.329
	2	-0.103	-0.143	-0.169	-0.218	-0.26	-0.27	-0.325	0.33	-0.339	-0.347
	3	-0.456	-0.502	-0.481	-0.483	-0.501	-0.52	-0.555	-0.62	-0.635	-0.646

Table 12 - Calculation of lignin peroxidase activity first culture

strains	ε (M cm^{-1})	Slope (min^{-1})	Sample volume (L)	LiP activity	
				µM per min	µM/L.min
Cast13	45160	0.025	0.5. 10^{-3}	0.11	221.61
Cast13 C	45160	0.002	0.5. 10^{-3}	0.012	24.09
RB111	45160	0.005	0.5. 10^{-3}	0.04	76.52
VBC 02	45160	0.004	0.5. 10^{-3}	0.14	294.71

Calculation lignin peroxidase activity:

Same calculation as laccase, with the change of the molar coefficient ε.

Table 13 - Specific lignin peroxidase activity

strain	LiP activity (U/L)	Total protein (mg/L)	Specific LiP activity (U/mg)
Cast13	221.61	4.87	45.47
Cast13 C	24.09	1.09	22.06
RB111	76.52	1.84	41.39
VBC 02	294.71	3.27	89.92

Specific LiP activity (U/mg) = LiP activity (U/L)/ Total protein (mg/L)

Table 14 - Absorbance at 651 nm for lignin peroxidase activity (second culture)

strain	5	10	15	20	25	30	35	40	45	60
Cast13	0.016	0.027	0.032	0.038	0.043	0.039	0.049	0.049	0.049	0.05
VBC02 (C)	0.212	0.277	0.242	0.316	0.292	0.236	0.215	0.176	0.232	0.212
RB111	0.017	0.028	0.035	0.044	0.047	0.055	0.057	0.057	0.06	0.058

Cast13 (C)	0.017	0.019	0.035	0.037	0.041	0.04	0.037	0.045	0.046	0.046
Vbc02	0.068	0.037	0.094	0.097	0.051	0.054	0.057	0.022	0.037	0.038

Table 15 - Absorbance at 270nm for Manganese peroxidase activity (first culture)

strain	0	1	5	10	15	20	25
Cast13	-0.007	-.0.002	-0.002	-0.003	-0.002	-0.001	-0.001
VBC02 (C)	0.004	0.001	0.001	0.001	0	0	0
RB111	0.003	0.002	0.002	0.001	0	0	-0.001
Cast13 (C)	0.007	0.007	0.005	0.002	0.001	0.001	0
VBC 02	0.005	0.000	-0.001	-0.003	-0.001	-0.001	0

Table 16 - Absorbance at 270nm for Manganese peroxidase activity (second culture)

strain	0	1	5	10	15	20	25
Cast13	0	-0.005	-0.005	-0.005	-0.006	-0.006	-0.006
VBC02 (C)	0	0.001	0.002	-0.001	-0.001	-0.001	-0.001
RB111	0	0.001	0.003	0.001	-0.001	-0.002	0
Cast13 (C)	0	-0.003	-0.006	-0.005	-0.002	-0.002	0.002
VBC 02	0.002	0.003	0.001	-0.001	-0.001	-0.002	-0.002

Table 17 - Calculation of molar coefficients of ABTS

ABTS concentration (mM)	0	0.001	0.002	0.003	0.004	0.005
OD at 405nm	0	0.065	0.115	0.166	0.218	0.274
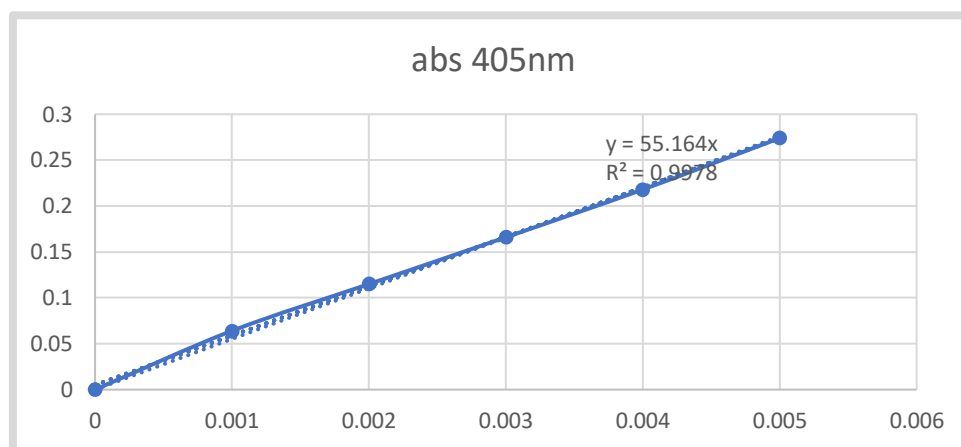
Figure 41 - Absorbance at 405nm for ABTS.

Table 18 - Calculation of molar coefficients of Azure B

Azure B concentration (mM)	0	0.005	0.007	0.008	0.01	0.015
OD at 651nm	0	0.374	0.57	0.596	0.698	0.917
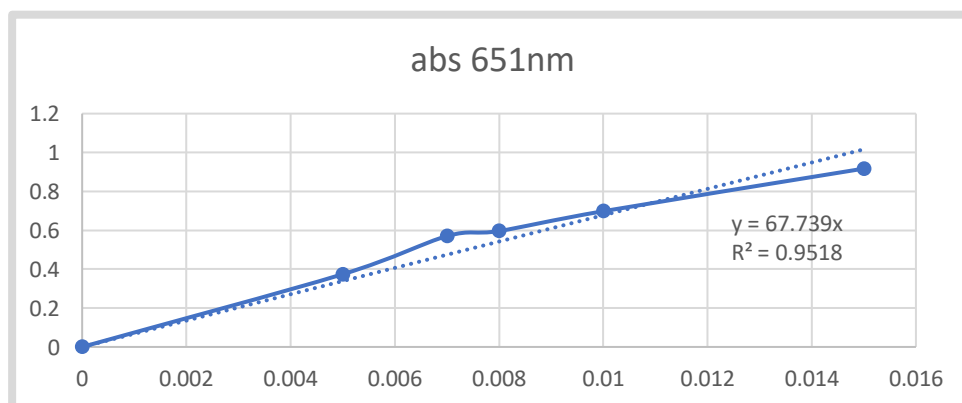
Figure 42 - Absorbance at 651nm for Azure B.

Appendix II : Calculation for Total protein content

Table 19 - Calculation of total protein concentration

BSA concentration (mg/L)	0.005	0.035	0.071	0.152	0.227	0.306	0.355
OD at 595nm	0.005	0.035	0.071	0.152	0.227	0.306	0.355
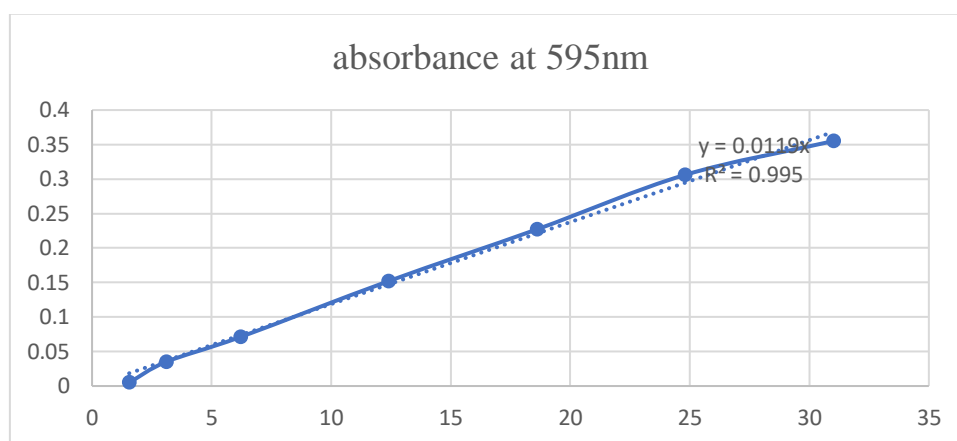
Figure 43 - Standard curve for protein analysis using BSA as standard

Table 20 - Calculation of total protein content for the first culture for each strain

strain / N°R	Cast13	VBC02	Cast13 C	VBC02 C	RB111
1	0.056	0.036	0.011	0.02	0.015
2	0.059	0.039	0.014	0.019	0.022
3	0.058	0.043	0.013	0.02	0.03
average	0.058	0.039	0.013	0.02	0.022
Protein content (mg/L)	4.87	3.28	1.09	1.68	1.84

Table 21 - Calculation of total protein content for the second culture each strain

strain / N°R	Cast13	VBC02	Cast13 C	VBC02 C	RB111
1	0.018	0.004	0.023	0.07	0.05
2	0.015	0.003	0.024	0.07	0.051
3	0.019	0.004	0.027	0.075	0.049
average	0.017	0.004	0.025	0.072	0.05
Protein content (mg/L)	1.43	0.34	2.10	6.05	4.20

Appendix III: Apple infection measures

Table 22 - Apples infection measures

n° of days	name of strain / N° R	Cast13 (mm)	VBC02 (mm)	Cast13 C (mm)	VBC02 C (mm)	RB111 (mm)
Day 4	**1**	7;10	10;10	9;10	7;7	8;9
	2	8;10	8;8	9;10	7;8	9;10
	3	7;8	9;10	9;11	5;7	6;10
	average	7;9	9;9	9;10	6;7	8;10
Day6	**1**	9;13	12;12	12;13	8;8	11;12
	2	10;13	10;11	11;12	9;9	11;13
	3	9;10	10;12	11;12	8;8	10;11
	average	9;12	11;12	11;12	8;8	11;12
Day10	**1**	15;18	19;19	16;17	10;10	16;17
	2	13;18	19;28	15;17	11;11	15;18
	3	12;12	16;18	16;16	9;9	12;13
	average	13;16	18;22	16;17	10;10	14;16
	Infection(Cercle) Area(mm^2)	165.13	314.16	213.82	78.54	176.71

Appendix IV: Lesions in Chestnut branches measures

Table 23 - Measures of lesions after 6 days inoculation

n° of days	name of strains / N°R	Cast13 (cm)	VBC02 (cm)	Cast13 C (cm)	VBC02 C (cm)	RB111 (cm)
Day 6	**1**	5.6;2.2	5.3;2.7	4;1.7	3.5;1.8	5.3;1.8
	2	4.5;1.9	5.4;2.5	3.6;1.4	3;1.6	4.1;1.8
	3	4.5;2.2	5;2.5	3.5;1.5	3.8;1.9	3.6;1.8
	average	4.9;2.2	5.2;26	3.7;1.5	3.4;1.8	4.3;1.8
	Lesion (Eclipse) area(cm^2)	8.47	10.62	4.36	4.81	6.08

Appendix V: BIOLOG microplate Data

Table 24 – testing the viability of the mycelium used in BIOLOG by inoculation and counting the number of sections appeared in Petri dishes.

Strains n° of sections/plate	1	2	3	Average	n° of sections/ml
Cast13	164	9	165	112.6	11260
VBC02	65	101	5	57	5700
Cast26	64	110	39	71	7100
Cast13 C	53	149	138	113.3	11330
VBC02 C	109	111	50	90	9000
Cast26 C	91	100	48	79.6	7960
RB111	75	106	10	63.6	6360
Serra05	85	51	15	50.3	5030
SR442	85	48	79	70.6	7060

Table 25 - Location of each carbon source in the FF microplate

	A	B	C	D	E	F
1	Water	Tween 80	N-acetyl-d-galactosamine	N-acetyl-d-glucosamine	N-acetyl-d-mannosamine	adonitol
2	Alpha-cyclodextrin	Bêta-cyclodextrin	dextrin	I-erythritol	D-fructose	L-fucose
3	Glusose-1-phosphate	glucuronamide	D-glucuronic acid	glycerol	glycogen	M-inositol
4	D-mannitol	D-mannose	D-melezitose	D-melibiose	Alpha-methyl-d-galactoside	Bêta-methyl-d-galactoside
5	D-ribose	salicin	sedoheptulosan	D-sorbitol	L-sorbose	stachyose
6	Gamma-amino-butyric acid	bromosuccinic acid	fumaric acid	Beta-hydroxy-butyric acid	Gamma-hydroxy-butyric acid	P-hydroxyphenyl-acetic acid
7	D-saccharic acid	sebacic acid	succinamic acid	succinic acid	succinic acid mono-mehtyl ester	n-acetyl-l-glutamic acid
8	glycyl-l-glutamic acid	l-ornithine	L-phenylalanine	L-proline	L-pyroglutamic acid	L-serine

	G	H	I	J	K	L
1	Amygdalin	d-arabinose	l-arabinose	D-arabitol	arbutin	D-cellobiose
2	D-galactose	D-galacturonic acid	gentobiose	D-gluconic acid	D-glucosamine	Alpha-d-glucose
3	2-keto-d-gluconic acid	Alpha-d-lactose	Lactulose	Maltitol	Maltose	maltotriose
4	Alpha-methyl-d-glusoside	Bêta-methyl-d-glucoside	palatinose	D-psicose	D-raffinose	L-rhamnose
5	Sucrose	D-tagatose	D-trehalose	turanose	Xylitol	D-xylose
6	Alpha-keto-glutaric acid	d-lactic acid methyl ester	L-lactic acid	D-malic acid	L-malic acid	quinic acid
7	alaninamide	l-alanine	L-alanyl-glycine	l-asparagine	L-aspartic acid	L-glutamic acid
8	l-threonine	2-amino ethanol	Putrescine	adenosine	Uridine	Adenosine-5´-monophosphate

Table 26 - Absorbance at 490nm for the strain VBC02c after seven days of incubation at 25°C.

	A	B	C	D	E	F	G	H	I	J	K	L
1	0	0.892	0	0.52	0.121	0.23	0.209	0.313	0.531	0.297	0.822	0.721
2	0.264	0.201	0.667	0	0.307	0.029	0.226	0.024	0.585	0.156	0.046	0.581
3	0.368	0	0.226	0.509	0.435	0.167	0.237	0.258	0.225	0.472	0.511	0.603
4	0.437	0.503	0.531	0.111	0.2	0.19	0.231	0.506	0.617	0.151	0.406	0.194
5	0.707	0.401	0.129	0.216	0.018	0.394	0.45	0.257	0.6	0.537	0.209	0.675
6	0.102	0.024	0.302	0.936	0.79	0.133	1.044	0.374	0.115	0.429	0.237	0.605
7	0.215	0.098	0.119	0.204	0	0	0.771	0.197	0.337	0.369	0.106	0.233
8	0.156	0.214	0.132	0.093	0.009	0.064	0.05	0	0.162	0.185	0.039	0.611

Table 27 - Absorbance at 490nm for the strain VBC02 after seven days of incubation at 25°C.

	A	B	C	D	E	F	G	H	I	J	K	L
1	0	0.533	0.029	0.626	0.055	0.105	0	0.02	0.528	0.442	0.888	0.206
2	0.379	0.116	0.241	0.014	0.807	0	0.428	0	0.794	0.099	0.173	0.205
3	0.739	0	0.583	0.044	0.578	0.003	0.018	0.049	0.611	0.334	0.267	0.663
4	0.747	0.335	0.351	0.1	0.019	0.514	0.34	0.424	0.481	0.219	0.157	0.148
5	0.522	0.028	0.168	0.536	0	0.128	0.035	0.27	0.951	0.607	0.183	0.866
6	0.107	0.088	0.731	0	0.01	0	0.279	0	0.092	0.717	0.504	0.873
7	0.119	0	0.353	0.363	0.36	0	0.445	0.469	0.109	0.136	0.406	0.423
8	0.321	0.032	0.025	0.111	0.1	0.017	0	0	0	0.25	0.043	0.707

Table 28 - Absorbance at 490nmm for cast13c after seven days of incubation at 25°C.

	A	B	C	D	E	F	G	H	I	J	K	L
1	0	0.644	0.056	0.441	0.185	1.297	0.006	0.972	0.673	0.502	0.451	1.638
2	0.326	0.484	0.544	0.372	1.177	0.717	1.314	0.676	1.074	0.617	0.182	0.814
3	1.058	0	1.275	0.683	0.509	0.255	0.321	1.165	0.714	0.854	0.452	0.534
4	0.607	1.314	0.961	0.542	0.131	0.197	0.534	0.469	0.547	0.904	0.436	0.489
5	1.763	0.182	0.909	1.19	0.153	0.401	1.091	0.874	0.619	0.838	0.99	1.424
6	0.405	0.339	0.942	0.032	0.172	0.359	0.326	0.675	0.174	0.427	0.496	0.881
7	0.507	0	0.346	0.441	0	0.221	0.507	1.368	0.74	0.664	0.159	0.415
8	0.058	0.168	0.05	0.104	0.222	0.761	0.259	0	0.099	0.322	0	0.537

Table 29 - Absorbance at 490nm for RB111 after seven days of incubation at 25°C.

	A	B	C	D	E	F	G	H	I	J	K	L
1	0	0.934	0.1	0.589	0.2	0.411	0.294	0.438	0.74	0.532	0.589	0.914
2	0.395	0.381	0.87	0.197	0.725	0.302	0.607	0.188	0.698	0.366	0.301	0.87
3	1.33	0.059	0.296	0.303	0.673	0.507	0.277	0.495	0.311	0.61	0.72	0.697
4	0.716	0.922	0.646	0.424	0.268	0.395	0.803	0.684	0.758	0.404	0.505	0.577
5	0.712	0.679	0.283	0.466	0.26	0.673	0.961	0.449	0.778	0.966	0.526	0.874
6	0.27	0.303	0.535	0.816	0.732	0.137	1.081	0.431	0.206	0.532	0.665	1.023
7	0.046	0.341	0.326	0	0.37	0.249	0.974	0.297	0.75	0.55	0.267	0.336
8	0.314	0.209	0.264	0.293	0.287	0.212	0.11	0	0.115	0.296	0.15	0.487

Table 30 - Absorbance at 490nm for Cast13 after seven days of incubation at 25°C.

	A	B	C	D	E	F	G	H	I	J	K	L
1	0	0.822	0.111	0.962	0.168	0.455	0	0.298	0.692	0.518	0.695	0.67
2	0.36	0.336	0.431	0.355	0.666	0.02	0.596	0.254	0.469	0.485	0.417	0.47
3	1.105	0	0.295	0.324	0.705	0.378	0.504	0.395	0.461	0.629	0.321	0.469
4	0.715	0.603	0.404	0.39	0.26	0.43	0.385	0.853	0.505	0.414	0.472	0.439
5	0.88	0.324	0.187	0.56	0.506	0.536	0.561	0.413	0.501	0.536	0.487	0.766
6	0.541	0.365	0.874	0.419	0.636	0.083	1.175	0.209	0.319	0.878	1.054	0.256
7	0.233	0.276	0.324	0.682	0.264	0.209	0.672	0.537	0.52	0.751	0.235	0
8	0.372	0.337	0.306	0.519	0.482	0.296	0.18	0	0.097	0.574	0.053	0.581

Table 31 - Average of absorbance at 490 for each chemical group after seven days of incubation at 25°C.

$AWCD_G$	Amines/Amides	Amino acids	Carbohydrates	Carboxylic acids	Miscellaneous	Polymers
VBC02 c	0.18	0.16	0.36	0.34	0.27	0.49
VBC02	0.17	0.16	0.34	0.26	0.22	0.37
Cast13c	0.19	0.41	0.75	0.46	0.38	0.50
RB111	0.29	0.32	0.57	0.44	0.46	0.65
Cast13	0.25	0.39	0.49	0.50	0.38	0.53

Table 32 - Margin of error in absorbance value for each chemical group.

AWCD$_G$	Amines/Amides	Amino acids	Carbohydrates	Carboxylic acids	Miscellaneous	Polymers
VBC02 c	0.12	0.03	0.03	0.08	0.07	0.13
VBC02	0.08	0.04	0.04	0.07	0.09	0.08
Cast13c	0.08	0.10	0.06	0.08	0.11	0.05
RB111	0.14	0.045	0.03	0.08	0.11	0.11
Cast13	0.11	0.05	0.03	0.08	0.10	0.1

Appendix VI: Statistical analyses of the results

Analysis of Variance Results

F-statistic value = 16.58834

P-value = 0.00021

Data Summary				
Groups	N	Mean	Std. Dev.	Std. Error
Group 1	3	8.0553	1.5002	0.8661
Group 2	3	10.5528	0.7121	0.4111
Group 3	3	4.474	0.755	0.4359
Group 4	3	4.796	0.9594	0.5539
Group 5	3	6.1259	1.2351	0.7131

ANOVA Summary					
Source	Degrees of Freedom DF	Sum of Squares SS	Mean Square MS	F-Stat	P-Value
Between Groups	4	76.62	19.155	16.5883	0.0002
Within Groups	10	11.5473	1.1547		
Total:	14	88.1672			

Figure 44 - Analyses of variance for chestnut branches results.

Analysis of Variance Results

F-statistic value = 6.19487

P-value = 0.00897

Data Summary				
Groups	N	Mean	Std. Dev.	Std. Error
Group 1	3	171.8712	52.428	30.2693
Group 2	3	314.748	106.855	61.6928
Group 3	3	205.316	7.3686	4.2542
Group 4	3	79.0633	15.7145	9.0728
Group 5	3	183.4558	52.6001	30.3687

ANOVA Summary					
Source	Degrees of Freedom DF	Sum of Squares SS	Mean Square MS	F-Stat	P-Value
Between Groups	4	85413.3197	21353.3299	6.1949	0.009
Within Groups	10	34469.397	3446.9397		
Total:	14	119882.7167			

Figure 45 - Analyses of variance for apple infection results.

Analysis of Variance Results

F-statistic value = 16.49974

P-value = 0.00364

Data Summary				
Groups	N	Mean	Std. Dev.	Std. Error
Group 1	3	841.7139	169.0095	97.5777
Group 2	3	477.1478	98.2073	56.7
Group 3	3	326.3108	9.5794	5.5307

ANOVA Summary					
Source	Degrees of Freedom DF	Sum of Squares SS	Mean Square MS	F-Stat	P-Value
Between Groups	2	421300.5973	210650.2987	16.4997	0.0036
Within Groups	6	76601.2995	12766.8833		
Total:	8	497901.8969			

Figure 46 - Analyses of variance for laccase activity results (first culture).

Analysis of Variance Results

F-statistic value = 1343.65454

P-value = 0

Data Summary				
Groups	N	Mean	Std. Dev.	Std. Error
Group 1	3	27048.3959	43.2326	24.9603
Group 2	3	5260.309	151.852	87.6718
Group 3	3	82957.0419	3394.568	1959.8548
Group 4	3	8519.5976	107.7596	62.215

ANOVA Summary					
Source	Degrees of Freedom DF	Sum of Squares SS	Mean Square MS	F-Stat	P-Value
Between Groups	3	11649114130.6387	3883038043.5462	1343.6545	0
Within Groups	8	23119264.2512	2889908.0314		
Total:	11	11672233394.89			

Figure 47 - Analyses of variance for laccase activity results (second culture).

Analysis of Variance Results

F-statistic value = 46.18904

P-value = 0.00023

Data Summary				
Groups	N	Mean	Std. Dev.	Std. Error
Group 1	3	45.469	3.444	1.9884
Group 2	3	41.3893	0.3774	0.2179
Group 3	3	81.3249	9.0599	5.2308

ANOVA Summary					
Source	Degrees of Freedom DF	Sum of Squares SS	Mean Square MS	F-Stat	P-Value
Between Groups	2	2897.1417	1448.5708	46.189	0.0002
Within Groups	6	188.1707	31.3618		
Total:	8	3085.3124			

Figure 48 - Analyses of variance for lignin peroxidase activity results.